The structural evolution of the Straumsnutane and western Sverdrupfjella areas, western Dronning Maud Land, Antarctica – implications for the amalgamation of Gondwana.

A.Bumby[1], G.H. Grantham[2] and N. Moabi[3]

[1] Department of Geology, University of Pretoria, Hillcrest, Pretoria, South Africa.

[2.] Department of Geology, University of Johannesburg, PO Box 524, Auckland Park 2006, South Africa.

[3.] Council for Geoscience, P/Bag X112, Pretoria, 0001, South Africa

Abstract

The study area is located across the Kalahari Craton - Maud Belt boundary in Dronning Maud Land (DML), Antarctica. The ~1100Ma Maud Belt in the east is situated where the ~900-600Ma East African and ~530-500Ma Kuunga Orogenies overlap. The Kalahari Craton cover in the west of the study area comprises ~1100Ma Straumsnutane Formation lavas in Straumsnutane.

In Straumsnutane early ~1100Ma low grade structures suggest top-to-the-NW deformation. Younger ~525Ma structures suggest conjugate top-to-ESE and WNW transport under low grade conditions. Western Straumsnutane and Ahlmannryggen do not show the same complex deformation, the intense deformation being restricted to NE Straumsnutane along the eastern margin of the Kalahari Craton.

In Sverdrupfjella, in the east, the Maud Belt is underlain by medium grade, deformed ~1140 Ma supracrustal gneisses and younger intrusions. Four deformation phases in the gneisses comprise D_1+D_2 with top-to-the-N and NW folds, D_3 top-to-the-S and SE folding and D_4 brittle faulting. Syn-D_3 emplacement of granitoid veins is inferred at ~490Ma.

Comparison of the deformation vergence of NE Straumsnutane with western Sverdrupfjella suggests D_1 in Straumsnutane is correlatable with D_1+D_2 Mesoproterozoic structures in western Sverdrupfjella. D_2 deformation in Straumsnutane can be correlated with D_3 structures and Cambrian-age granites in Sverdrupfjella.

D_2 deformation in eastern Straumsnutane and D_3 in western Sverdrupfjella are inferred to have occurred in a mega-nappe footwall, implying the Ritscherflya Supergroup cratonic cover in eastern Straumsnutane was partially submerged in the footwall, the mega-nappe formed during Gondwana amalgamation, involving collision between N and S Gondwana in the Kuunga Orogeny, ~530-500Ma ago.

INTRODUCTION.

Western Dronning Maud Land (WDML) is strategically located in an area where the inferred extents of the East African Orogeny (EAO) and the Kuunga Orogenies (KO) overlap (Figures 1 and 2). The processes and timing of these orogenies are inferred to have contributed to the amalgamation of Gondwana and consequently an understanding of the nature of deformation in the study area (Figure 2) can contribute to an insight into the interpreted configurations and timing of Gondwana amalgamation.

East African Orogeny

The EAO was originally proposed by Stern (1994; 2002) to extend from the Arabian-Nubian shield to northern Mozambique and was inferred to involve a Wilson cycle from ca. 900 Ma to ca. 600 Ma in which East Gondwana collided with West Gondwana with the opening and closure of the Mozambique Ocean. Jacobs et al., (1998) proposed a geographical extension to the EAO, to CDML Antarctica and a geochronological extension to include ca. 500 Ma age deformation in DML. The

age of the deformation was constrained by K-Ar and Ar-Ar dating of mica and amphibole in Heimefrontfjella (Jacobs et al., 1995,1996; 1997, 1999). Jacobs et al., (1998, 2003a,b,c and 2004 and subsequent papers) concluded that an intercontinental scale transpressional sinistral shear structure for the East African Antarctic Orogen was involved in the amalgamation of East and West Gondwana, stretching from central East Africa to Heimefrontfjella (Figure1,2). Within the study area (Figure 2), a suture was inferred along the west as part of the large scale shear structure. The nature of the suture in the study area was not defined however, but was inferred to be sinistral northwards in southern Africa and dextral to the south in Heimefrontfjella. The positioning of the sutures of the intercontinental scale sinistral shear along the E and W were reportedly inferred from earlier publications of Shackleton (1996), Grunow et al., (1996) and Wilson et al. (1997). The sutures defined by Shackleton (1996) along the west, comprise orthogonal W to WNW directed thrust fault zones toward cratonic blocks in central and southern Africa and WDML with no strike-slip component defined. Shackleton (1996) recognised top-to-the-SE thrust zones in the Lurio Belt and Sri Lanka. Wilson et al., (1997) and Grunow et al., (1996) discuss various permutations of sutures in southern Africa and Antarctica and suggested an eastern suture linking the Lutzo-Holmbukta area with the Shackleton Range across Antarctica, separating a Pan-African Belt in the west from an Antarctic Craton in the east. Fitzsimons (2000) similarly inferred Cambrian-sutures through the Sri Lanka-Lutzo Holmbukta areas and a separate one in the Shackleton range area but did not support continuity between the two areas. Mieth and Jokat (2014) conclude that there is no aeromagnetic geophysical data in support of an inferred suture linking Lutzo Holmbukta with the Shackleton Range. Fitzimmons (2000) reflects a dominant 650-550Ma orogen across the Nampula Terrane of northern Mozambique however subsequent data from that area (Macey et al., 2010; Bingen et al., 2009; Grantham et al., 2008) have reported a dominantly Mesoproterozoic basement which has a metamorphic overprint of <570 Ma with ages >600 Ma only recorded in granulite grade klippen (Macey et al., 2013 ; Grantham et al., 2013).

Structural data published from Heimefrontfjella and Gjelsvijfjella (Jacobs et al., 1996, 2003a), both areas in DML adjacent to the study area, contributed to the inferred EAO extension to Heimefrontfjella(Figure 2). In Heimefrontjella, a dextral oblique strike slip curvilinear shearzone in the north reportedly becomes a frontal ramp with dip-slip in the south (Jacobs et al., 1996). Late D3 shearing of Pan African ca. 500 Ma age is inferred as having a top-to-SE sense of shear. At this locality, the dextral sense of shear is inferred to contribute to the escape southwards of a smaller crustal block (Jacobs and Thomas, 2004). Age constraints from these structures are reported in Jacobs et al., (1995,1996; 1997, 1999) with Ar-Ar ages on biotite being typically ca. 500 Ma and hornblende ages of ca.550-500 Ma except for the Kottas Terrane with hornblende ages of ca. 1000 Ma.

In Gjelsvikfjella, at the western end of the CDML (Figure 2), Jacobs et al., (2003b) recognised two events with an early dilational event at ca. 558 Ma and a later event between 530 and 490 Ma with limited associated deformation. Whereas the association with deformation with these events was reported, the deformation trajectory directions were not reported. Significantly, a WNW-ESE oriented thrust fault with top-to-the S and SSW stretching lineations was described however no strike-slip sinistral deformation was reported. Baba et al., (2015) report a shear zone with location and orientation in Gjelsvikfjella similar to that of Jacobs et al., (2003b), and describe granulites in the hanging wall with ages between ca. 598 Ma and 633 Ma, indicating that the S to SSW thrusting is younger than ca. 598 Ma. Jacobs et al., (2003b) reported granitoid and limited basic magmatism in Gjelsvikfjella and further east in CDML and Mozambique (Jacobs et al., 2008) which they described as being late tectonic and related to extensional post orogenic collapse related to delamination of the orogenic root of the EAO. The direction of inferred extension was not defined. Structural trend maps from CDML are described in Jacobs et al (1998, 2003c) showing an ENE striking shear in the Orville Shear Zone with sinistral sense of shear inferred to be of Pan African

age (Bauer et al.,2003). The Orvinfjella Shearzone has been correlated with the Namama Shearzone (Cadoppi et al., 1987) in Mozambique (Grantham et al., 2003) where it terminates within the Nampula Complex and consequently does not represent a suture.

Kuunga Orogeny

In a detailed study of geochronological data, Meert (2003) proposed a marginally younger orogenic event (ca. 570-530 Ma) over printing the EAO and termed it the Kuunga Orogeny (KO) (Figure 1). The KO was interpreted as extending from the Damara in Namibia, through the Zambesi belt, across northern Mozambique, into Dronning Maud Land (DML), Antarctica, through southern India and Sri Lanka, south of Enderby Land, Antarctica, and into western Australia (Figure 1). In support of the Kuunga Orogeny, Grantham et al., (2008), proposed a continent-continent collision setting between N and S Gondwana, based on correlated lithological, structural, geochronological and metamorphic P-T conditions between southern Africa, DML and Sri Lanka. The collisional model proposed N. Gondwana being thrust southwards over S. Gondwana involving a mega-nappe structure with tectonic transport of up to ca. 500 km between N. Mozambique and Dronning Maud Land (Figure 1 and 2). Fundamental to the mega-nappe model are (a) the significance of klippen structures along the northern margin of southern Gondwana comprising the Naukluft Nappes of the Damara Orogen in Namibia, Urungwe Klippen (N. Zimbabwe), Mavhuradohna Complex (NE Zimbabwe), Mugeba and Monapo Klippen (Mozambique) and Kataragama Klippen (Sri Lanka) (Figure 1, Grantham et al., 2008) and (b) the recognition that the lithologies in CDML are lithologically and geochronologically dissimilar to those of the Nampula Complex (Figure 2) in Mozambique but similar to those of the Namuno Terrane, north of the Lurio Belt (Figure 2) (Grantham et al., 2008). The locations of the latter three klippen, correlated with the Namuno Complex, are shown in Figure 2 and imply that the Nampula Complex (Mozambique) and Vijayan Complex (Sri Lanka) were in the footwall of a nappe complex, the hanging wall now largely

removed by erosion. The geology of CDML was also inferred to be allochthonous, being correlatable with rocks from the Namuno Terrane of northern Mozambique (Grantham et al., 2008). The wider and larger extent of the CDML nappe structure was inferred to result from lower erosion rates in ice covered Antarctica (Grantham et al., 2008), recognising that the Antarctic ice sheet has inferred to have grown at least since 35Ma (Rose et al., 2013) as well as loading of the continent under the Antarctic ice sheet (Grantham et al., 2008) recognising the Antarctic ice sheet being up to 5 kms thick locally. In contrast, the Nampula Complex has experienced higher rates of erosion and uplift, reflected by fission track data, since Gondwana breakup ca. 190Ma ago being located in a subtropical climate (Daszinnies et al., 2009). Grantham et al., (2013) described further details of lithological, geochronological and metamorphic similarities between the Monapo Klippen in Mozambique and eastern Sor Rondane in DML, Antarctica, in support of the mega-nappe model, and extending it onto the Antarctic continent. Grantham et al., (2019) broadened the longitudinal extent of the mega-nappe in the west to Gjelsvikfjella and eastern Sverdrupfjella from the original inference of CDML in Grantham et al., (2008) and constrained the latitudinal extent of the mega-nappe in WDML to Sverdrupfjella and N. Kirwanveggan, based on new $^{40}Ar/^{39}Ar$ age and Nd/Sr whole rock radiogenic isotope data. The $^{40}Ar/^{39}Ar$ cooling ages from biotite and hornblende in Sverdrupfjella and Kirwanveggan demonstrate that ~500Ma metamorphism and deformation did not extend to southern Kirwanveggan and beyond to Heimefrontfjella, indicating that extension of the EAO, along the eastern margin of the Kalahari Craton was invalid, recognising that Heimefontfjella is separated from Kirwanveggan by sedimentary basins of ca 550Ma old Urfjell Group and overlying Karoo age sedimentary rocks in Kirwanveggan (Figure 2) . Grosch et al., (2015) and Grantham et al., (2019) conclude that east Sverdrupfjella has been tectonically emplaced over West Sverdrupfjella at mid to late Pan African times. Grantham et al., (2019) demonstrate that east Sverdrupfjella is isotopically distinct from west Sverdrupfjella, having juvenile protoliths with TDm ages <ca. 1800Ma, in contrast to western

Sverdrupfjella with TDm ages >ca. 2000Ma. Syntectonic granitic veins intruding both E and W Sverdrupfjella, with isotopic characteristics consistent with being sourced from the older W Sverdrupfjella basement crust, with ages of ca. 490Ma, show top-to-the-SE sense of shear during emplacement with extensional and compressional displacements in a simple shear setting (Grantham et al., 2019).

The term Maud Belt was proposed by Groenewald (1993) referring to the lithologies underlying WDML which were assumed to be Mesoproterozoic in age, based on the available data. The extent of the Maud Belt has been revised in Mendonidis et al., (2015) in which it is now recognised that the Maud Belt is marginally younger at ca. 1140 Ma than the Natal-Namaqua Belts of southern Africa at ca. 1225 Ma (Grantham et al., 2011), the boundary between the two belts being located in Heimefrontfjella. Northwards in Gondwana, the Maud Belt, now recognised as being exposed in W Sverdrupfjella (Grantham et a., 2019), is correlated with the Barue Complex and its extention to the Nampula Complex in N. Mozambique (Grantham et al., 2011) (Figure 2). Consequently in Antarctica, the ca. 1140 Ma Maud Belt is restricted to western Sverdrupfjella with eastern Sverdrupfjella being correlated with the CDML domain (Grantham et al., 2019). Extensions of the Maud Belt are however inferred to extend through the Barue and Nampula Complexes of N. Mozambique into the Vijayan Complex in Sri Lanka (Figure 2)(Grantham et al., 2008; 2011, Wai-Pan et al., (2017).

In proposing the mega-nappe model it was recognised that the inferred distance over which the nappe was emplaced, varied significantly. Whereas the distance that the Kuunga nappe is thought to have covered between northern Mozambique and DML is ca. 500-600 km, the emplacement distance related to the Urungwe Klippen, emplaced onto the northern Zimbabwe Craton in Zimbabwe is significantly less and ca. <100 km (Grantham et al., 2008). The differential in distance between the two areas is channelled along the eastern margin of the Kalahari Craton and the

Maud Belt to the east (Figure 2), inferring a top-to-the-SE, dextral sense of shear for the hanging wall of the nappe at ca. 530-500 Ma, east of the Kalahari Craton with the Maud Belt of western Sverdrupfjella and its correlatives in Mozambique and Sri Lanka representing the footwall (Figure 2).

The structural data described below, collected from the Straumsnutane area in 2012/2013, were aimed at determining whether any structures could be identified there, that could be consistent with the nappe model extending onto the Kalahari Craton. The structural data described below from Sverdrupfjella were collected during PhD studies (Grantham, 1992) and were summarised in Grantham et al., (1995; 2008) and were an integral component used in the formulation of the mega-nappe model in Grantham et al., (2008). In describing and discussing the structural evolution of the study area, there has been debate as to the extent and timing of the deformation history involving the description and identification of both Mesoproterozoic and Neoproterozoic/ Cambrian (Pan African) deformation phases and whether these are recognised in the various areas and can be differentiated structurally and geochronologically. Consequently, in the descriptions and discussions below, the characteristics of both phases of deformation are described.

GEOLOGY OF THE STUDY AREAS

Ahlmannryggen and Straumsnutane

The geology of the study area in western Dronning Maud Land, Antarctica comprises two geological terranes with a cratonic area located west of the Jutulstraumen Glacier and a medium grade metamorphic terrane east of the glacier (Figure 3). The cratonic terrane is underlain by the ~3067 Ma old Annandagstoppane Granite (Marschall *et al*., 2010) which is overlain by the Ritscherflya Supergroup (Wolmarans and Kent, 1982) comprising a volcano-sedimentary sequence intruded by basic sills of the Borgmassivet Suite. The Ritscherflya Supergroup comprises the

sedimentary Ahlmannrygen Group and volcanogenic Jutulstraumen Group (Wolmarans and Kent, 1982). The Straumsnutane Formation basaltic andesites are inferred as forming the top most sequence of the Jutulstraumen Group, overlying the Fasettfjellet Formation (Watters *et al,* 1991, Watters 1972).

The Straumsnutane area of western Dronning Maud Land (Figure 4) is underlain by basaltic andesites and subordinate intercalated sedimentary rocks of the Straumsnutane Formation. The age of the Straumsnutane Formation is best constrained by the study of the detrital zircons of the sedimentary Ahlmannryggen Group which underlies the Straumsnutane lavas, conducted by Marschall *et al.,* (2013) and by the age of Borgmassivet Suite intrusions. Marschall *et al.,* (2013) concluded that the depositional age of the Ahlmannryggen Group is <1125 Ma whereas Hanson et al., (2006) report an age for the Borgmassivet Suite of 1107 ± 2 Ma. The data reported by Marschall *et al.,* (2013) also reflects that many zircons analysed were discordant and suggested a lower intercept age of ~550Ma, interpreted as resulting from low grade metamorphism related to the "Pan African" amalgamation of Gondwana. Other attempts at constraining the age of the Straumsnutane lavas using Rb/Sr methods suggested an age of 848± 28Ma (Eastin *et al.,*1970) with a model age of 1664 ± 35Ma. Watters *et al.,* (1991) reported Sm/Nd T_{chur} model ages of between 1300 and 1620 Ma. That the model ages are significantly older than the age of ~1125Ma, suggests that the lavas have probably been contaminated by older crust in their genesis. Peters *et al.,* (1990) reported K-Ar ages of 526±11Ma and 522±11Ma from syntectonic white mica from a mylonite zone at Utkikken, N. Straumsnutane. Peters (1989) concluded that the white mica had grown syntectonically with K metasomatism, with the mica displaying a strong preferred planar orientation in the shear planes. The radiogenic isotope and whole rock major and trace element chemistry of the Straumsnutane Formation lavas have been described by Moabi et al., (2017) who concluded that the chemical compositions of the Straumsnutane basaltic andesites indicated that

they are comparable to and correlatable with the Borgmassivet Intrusive Suite in western Dronning Maud Land as well as the Espungaberra Formation basaltic andesites and Umkondo sills in southern Africa, all forming part of the ~1100Ma Umkondo Large Igneous Province (Hanson et al., 2006)

The most detailed study of the structures of the Ahlmannryggen is that of Perritt and Watkeys (2003) who concluded that gentle folding and jointing were the dominant structures. They concluded that the Ahlmanryggen Group showed open folding with near horizontal fold axes, trending NE to ENE. From a detailed study of joint patterns in the Borgmassivet and Ahlmannryggen areas, they concluded that the deformation, had originated from Pan-African-aged sinistral strike-slip faulting along the boundary between the cratonic Grunehogna and Maud metamorphic terranes. Watters *et al.* (1991) described intense shearing dipping 65-70^{o}ESE at the eastern nunataks in Straumsnutane, with the intensity of the shearing dissipating westwards. They reported fairly tight NE-trending folds overturned to the SE in NE Straumsnutane. Spaeth (1987) and Spaeth and Fielitz (1987) provide the most comprehensive structural studies of Straumsnutane to date. Spaeth (1987) described strong SE dipping planar fabrics, as well as top-to NW thrust faulting, referring specifically to an exposure (see Figure 10 later) at Snokallen. He also provided a description of conjugate mesoscale faulting with slickenside planes, dipping dominantly to the SE.

Western Sverdrupfjella

Western Sverdrupfjella is underlain by highly deformed and metamorphosed ca. 1140 Ma Mesoproterozoic gneisses which have been intruded by Cambrian age granite veins and pegmatites, metabasic dykes of uncertain age and Jurassic alkaline complexes and dolerite dykes. The chemistry, structural geology and metamorphic history of the gneisses and intrusions of

western Sverdrupfjella have been described in an unpublished PhD thesis (Grantham, 1992). Grantham et al., (2006) and Grosch et al.,(2007) describe the chemistry and age of metamorphosed mafic dykes of varying age. Grantham et al., (2006) report a deformed mafic dyke, which transects migmatitic layering in tonalitic gneisses, with an upper intercept SHRIMP U/Pb zircon age of ca. 900 Ma and lower intercept age of 523 ± 21 Ma. Harris et al.,(1991), Harris and Grantham, (1993), Riley et al., (2005) and Grantham (1996) describe the geology and chemistry of Jurassic dykes and the alkaline complex at Straumsvola. Grantham et al., (2011), described tonalitic gneisses from western Sverdrupfjella, Kirwanveggan and northern Mozambique, with ages of ca. 1140 Ma, in support of correlating the Maud Belt, Dronning Maud Land and the Barue Complex of central Mozambique. Grosch et al.,(2015) studied the metamorphic P-T conditions between western Sverdrupfjella and the eastern margin of the Ahlmanryggen and concluded that the physical conditions at ca. 500Ma were ca. 700^{o}C and 0.9GPa and ca. 350^{o}C and 0.3GPa respectively. In addition, they concluded that western Sverdrupfjella was separated from eastern Sverdrupfjella by a thrust fault zone, however no structural data was described in support of the conclusion. The structural history of western Sverdrupfjella has been briefly described by Grantham et al., (1995) and Grantham et al., (2008).

Recognising that detailed structural studies from Straumsnutane and Sverdrupfjella have not previously been reported, this paper is aimed at documenting and interpreting the structural geology of Straumsnutane and western Sverdrupfjella and placing these data in a broader tectonic setting related to the amalgamation of Gondwana.

FIELD DESCRIPTION

Straumsnutane

Watters *et al.,* (1991) provided the most detailed description of the volcanic rocks of the Straumsnutane Formation. They reported flow thicknesses ranging from ~1 to >50m with rocks being variably massive to varying degrees of amygdale development (Figure 5a). Pillow lavas were estimated to form ~10% of the ~850m thick sequence. The pillows typically form discrete ellipsoidal bodies with shearing along the inter-pillow groundmass (Figure 5b). At one locality deformed columnar jointing is preserved (Figure 5c). Pillowed sequences typically grade upwards into massive lava flows (Watters *et al.,* 1991). At many localities the interpillow areas are filled with white quartz and calcite. Thin sedimentary beds are sporadically intercalated with the lava. Nunataks along the eastern margin typically have strong planar fabrics which have destroyed primary features except amygdales. The latter are commonly elongated defining linear features typically oriented parallel to mineral and stretching lineations when developed at the same localities. Primary structures are better preserved and recognised in nunataks away from the Jutulstraumen Glacier and include volcanic breccias (Figure 5d), cooling cracks (Figure 5e) and ropy lava textures (Figure 5f). At some localities large ovoid quartz lenses are seen. The origin of these is uncertain and may be large vesicle fillings. Some of these structures have cores of lavas around which a quartz band is developed (Figure 6a).

Primary minerals preserved in these rocks include clinopyroxene and andesine plagioclase. The rocks are extensively altered with chlorite, white mica and epidote being common (Figures 6d, e and f). Amygdales are filled with recrystallised quartz, zeolites and calcite (Figure 6c&d). Serpentine pseudomorphs after olivine are seen in some samples from more basaltic compositions. Retrogressive prehnite and pumpellyite were described by Moabi et al., (2017). Mylonitised zones have strong planar fabrics (Figure 6b). A detailed study of the chemistry of the lavas shows they are basaltic andesites whose genesis has probably involved mixing between a MORB-like basaltic magma with evolved Achaean crust at depth (Moabi et al., 2017).

Structural Data

Structures observed in the field can be grouped into folds, thrust faults and associated structures, small mesoscale slickensided fault planes and vein arrays. The most common structures in the field comprise planar foliations, slickensided fault surfaces with strong lineations, and quartz veins. The latter commonly form multiple generational en-echelon arrays. Less common structures include mineral and stretching lineations, and mesoscale folds.

Primary structures defining layering are rarely observed with the clearest examples being seen at Snokjerringa, the nunatak most far removed from the Jutulstraumen in the west (Figure 4) and from Snokallen. Pi pole plots of primary layering, the data for which are mostly derived from Snokjerringa, define a π girdle oriented NW-SE (Figure 7a), consistent with folding about a near horizontal NE-SW oriented fold axis. The SE dipping layers dip shallowly to moderately (~45-50^{o}) whereas the NW dipping layers dip shallowly, suggesting slightly asymmetric folding (Figure 7a) and a NW dipping, SE vergent axial plane. This folding has the same top-to-SE folding orientation described by Watters et al. (1991). In contrast, schistose planar foliations in the area are strongly developed in the east along the edge of the Jutulstraumen Glacier and are typically steep, dipping dominantly to the south east (Figure 7b), with primary structures no longer recognisable. Sparse mineral and stretching lineations observed on the foliation planes similarly plunge steeply to the SE (Figure 7c).

The nunatak group Trollkjellpiggen (Figure 4) can be divided into an east and a west exposure. At the most southerly exposure of the west nunatak (locality 7, Figure 4), a well-developed south-easterly dipping mylonite layer, ca. 0.7m thick, is exposed over ca. 25m before disappearing under scree rubble (Figure 8a). Adjacent to the mylonite, the rocks have a strong planar fabric,

discordant to sub-parallel to the mylonite layer (Figure 8d) as well as several small splay offshoots (Figure 8e). One of these splay offshoots shows clear top-to NW drag features with truncation of a ~10cm ovoid quartz lens (Figure 8e). Within the mylonite band itself, flow folds with top-to-the west geometry, are defined by pale green epidote-rich layers (Figure 8b) as well as localised truncations of internal layering (Figure 8c). Structural data from this splay offshoot fault are shown in Figure 7f which shows steep SE dipping planar fabrics, shallower SE dipping mylonitic layering and steep to shallow, S plunging lineations. Locally, the mylonite zone is truncated by folded sub-horizontal quartz veins indicating that quartz veining post-dated the mylonitisation.

In a small windscoop, ca.15m E from the mylonite band, multiple phases of quartz en-echelon vein systems are seen (Figure 9). Four relative ages of veins can be identified from cross cutting relationships (Figure 9 top left and right). The oldest phase of veins is oriented near vertical and shows weak folding (Figure 9 top left and right). In addition, the filling of the oldest vein does not show any preferred crystal orientation growth. In contrast, the younger vein phases show fibrous quartz growth with the fibres mostly straight and orthogonal to vein margins, with curvilinear fibre growth being seen locally. The younger veins dip either to the east or are near-horizontal with some of the veins being weakly sinusoidal. The vein array envelope at this locality dips westwards at ~45^{o} (Figure 9 bottom). In those veins showing quartz fibre fills, the orientation of the quartz fibres is dominantly near vertical with minor steeply west dipping fibres or curvilinear fibre growth (Figure 9 top right). The dip of the vein array, with the weakly sinusoidal shapes, as well as the apparent rotation of veins from near horizontal to near vertical with increasing age, suggest a top-to-the east geometry as shown in Figure 9 (Bons *et al.,* 2011) with vein orientations being progressively rotated in an anti-clockwise manner.

In the exposure on the southern wall of Snokallen (locality 114, Figure 4 and Figure 10 top) a well-defined thrust fault is evident with a top-to-west geometry, similar to the structure at SW Trollkjellpiggen shown in Figure 8. This structure was previously described and similarly interpreted in a sketch by Spaeth (1987). In the exposure, it is clear that the layering of overlying sedimentary and pillowed volcanic rocks are not disrupted by the thrust fault (Figure 10 top) suggesting that the deformation was syn-depositional. This inference would consequently constrain the top-to-the west deformation as being of Mesoproterozoic age. A large mesoscale scale fold with similar WNW vergent axial plane and coarse axial planar-oriented veins (nunatak 1090 Figure 4, Figure 10 bottom) has a similar top to the northwest sense of deformation to the mylonite at Trollkjellpiggen and thrust fault at Snokallen. These large mesoscale structures suggest top-to-NW deformation during the Mesoproterozoic volcanism and sedimentation in Ahlmanryggen.

At almost all nunataks in the area, quartz-rich slickensided fault surfaces with varying attitudes and senses of movement with strong lineations are seen (Figure 11a). Most are typically coated by pale-green amorphous epidote-rich layers and quartz. These slickensided surfaces truncate the planar fabrics at some localities as well as the mylonite zone in Figure 8, indicating that they appear to be the youngest generation of structures in the area. Their attitudes are shown in Figure 11(b), which shows WNW- and ESE-dipping slickensided fault planes, with low angles of dip generally. Hanging wall movement is almost invariably upwards or reverse, with only very few examples of oblique or strike-slip fault movement. Application of the right dihedral method (Angelier and Mechler, 1976) was undertaken using Fabric 8 software for paleostress analysis, using measurements from various individual nunataks and from the area as a whole. The data suggests that the slickensides have resulted from brittle shear with a sense of shear towards both the WNW and ESE (Figure 11 b-e) with σ_1 plunging gently towards the WSW. It is possible that

these relatively young structures are similar in age to the cross-cutting en-echelon quartz veins, which suggested east-vergent geometry, and thus they are inferred to have formed part of the same deformational phase, having similar senses of shear orientation, and similarly orientated paleostress ellipsoids. Peters *et al.,* (1990) reported K-Ar ages of 526±11Ma and 522±11Ma from syntectonic white mica from these structures.

Western Sverdrupfjella

Grantham et al., (1995) subdivided Sverdrupfjella into eastern and western areas (Figure 3 and 12). Subsequent analysis of published radiogenic isotope data from the basement gneisses in Sverdrupfjella has shown that nunataks east of and including Fuglefjellet have significantly more juvenile Nd isotopic signatures ($\varepsilon Nd_{(t)}$ between ~3 to -3) compared to gneisses to the west ($\varepsilon Nd_{(t)}$ between ~-6 to -15) (Grosch et al., 2015, Grantham et al., 2019). In addition, thrust faults with top-to-the-NW sense of displacement are also recognised in most nunataks east of and including Fuglefjellet (Grantham et al., 1995) with none recognised in west Sverdrupfjella, west of Fuglefjellet. Pressure-temperature estimates indicate that east Sverdrupfjella is characterised by isothermal decompression paths from ca. 1.4 GPa down to ca. 0.9 GPa (Pauly et al., 2016; Groenewald and Hunter, 1991; Board et al., 2005). In contrast P-T estimates from west Sverdrupfjella infer maximum pressures of 0.8-0.9 GPa and have a loading anticlockwise P-T path (Grantham 1992, Grantham et al., 1995; Grosch et al., 2015). Recognising the higher pressures in east Sverdrupfjella and the general SE dipping structural train between east and west Sverdrupfjella, an inverted P-T gradient is apparent with higher pressure assemblages in east Sverdrupfjella overlying lower pressure rocks in west Sverdrupfjella. Consequently it is inferred that east Sverdrupfjella is allochthonous over west Sverdrupfjella with the boundary between east and west Sverdrupfjella (Figure 12) being of a tectonic, structural nature. Grosch et al., (2015) have also inferred east and west Sverdrupfjella being separated by a tectonic boundary with East

Sverdrupfjella being emplaced tectonically over west Sverdrupfjella. No structural data are provided by Grosch et al., (2015) in support of the nature of the tectonic boundary.

Western Sverdrupfjella is underlain by Mesoproterozoic supracrustal gneisses, granitic and metabasic veins and Jurassic alkaline complexes and dolerites. The supracrustal gneisses are subdivided into a Grey Gneiss Complex and Banded Gneiss Complex (Grantham et al., 1995) with the Grey Gneiss Complex being interpreted as being dominantly meta-andesitic in composition, typical of island-arc compositions. The Banded Gneiss Complex comprises interlayered quartzofeldspathic to metabasic gneisses, including subordinate rare calc-silicates and semi-pelitic Grt-Bt gneisses. The age and chemistry of the Grey Gneiss Complex are described in Grantham (1992), Grantham et al., (1997) and Grantham et al., (2011) with a SHRIMP zircon crystallisation age of ~1140 Ma and metamorphic rim overprints of ~600-514Ma. Rocks with composition and mineralogy similar to the Grey Gneiss Complex, but not necessarily of the same age, are subordinate at Fuglefjellet and absent from nunataks east of Fuglefjellet.

Structural data

Grantham et al., (1995) and Grantham (1992) have described the structural history of Sverdrupfjella and Kirwanveggan and western Sverdrupfjella respectively, providing regional overview summaries. The data described below from western Sverdrupfjella, are from an unpublished PhD thesis (Grantham 1992) and represent detailed structural measurements from individual localities which were summarised in Grantham et al., (1995) and Grantham et al., (2008). Four phases of deformation were reported from western Sverdrupfjella. Deformation phases D_1 and D_2 were described as comprising tight isoclinal recumbent fold phases with top-to-the-N and NW vergences (Figures 13a,b and c and Figure 14a). D_1 folds were recognised as having

axial planar foliations (Figure 13a) whereas D_2 folds were recognised in examples where the planar fabric developed during D_1 is folded about D_2 fold axes (Figure 13b and 13c).

Open folds typical of D_3 are also evident in Figures 13b, c, d and e. D_3 folds were described mostly as open asymmetric, synformal folds with top-to-the-S or SE vergences (Figures 14 a, b,c,d,e,f,g) with N to NW dipping axial planes and near horizontal E to NE plunging fold axes (Figures 14a-g and 15 a-f). In Figures 14c,f and g, the exposures are intruded by thin (up to 10m thick) SE dipping granitic veins of Dalmatian Granite and pegmatite (Grantham et al., 1991) which are typically orientated at high angles or perpendicular to the axial planes of these folds. The granite veins are dilational structures whose pole orientation can be inferred to parallel the σ_3 axis of strain, prevalent during their intrusion. This orientation/relationship is also observed in Figure 14e where a metabasic layer is boundinaged/segmented with the individual blocks separated by pegmatitic veins whose dilation direction is perpendicular to the axial plane of the F_3 fold. The vergences of the folds in Figures 14 a,b,c,e,f and g permit the inference of a top-to-the-South and SE tectonic movement.

Figure 15 summarises measurements of folds from various localities in western Sverdruprupfjella. Figure 15a represents measurements of the fold shown in Figure 14c and 14d and shows a ca. N-S π girdle, defined by S_0+S_1 planar fabrics and defines a shallow plunging fold axis toward ENE. The axial plane dips steeply N. Figure 15b represents measurements from the large fold shown in Figure 14f and shows a ca. N-S π girdle defined by S_0+S_1 planar fabrics and define a near horizontal fold axis plunging toward E. The axial plane dips at ca. 45^o toward N. Figure 15c represents the measurements from the large fold shown in Figure 14g at Roerkulten and shows a ca. N-S π girdle defined by the granite contact and S_1 planar fabrics which define a shallow plunging fold axis toward W. The axial plane dips steeply N. Figure 15d shows measurements from the fold shown in

Figure 14e. The layering S_0+S_1 dips dominantly N with axial planes dipping at ca. 45^o toward N and an almost horizontal fold axis plunging E. Figure 15 e and f show measurements from the fold shown in Figure 13d where an amphibolite dyke, described in Grantham et al., (2006) is folded. The dyke has a weak axial planar fabric developed which dips ca. 45^{o}NW. The dyke and planar fabrics in the country rock define a NW oriented π girdle with near horizontal NE oriented fold axes. Common to all the structural measurements of the D3 folds described here in Figures 14 and 15, are folds with N to NW dipping axial planes, consistent with top-to-the S and SE transport, crosscut by SE dipping dilational granite sheets.

In east Sverdrupfjella, structures associated with the Dalmatian Granite veins, have similarly been interpreted to represent the syntectonic emplacement of the granite with a top-to-the-SE sense of shear (Grantham et al., 1991, 2019). These structures include mesoscale brittle reverse faults displacing granite vein margins but not affecting the vein intrusions as well as extensional structures displacing earlier vein intrusions along the plane of intrusion of the granite sheets (Byrnes, 2015, Grantham et al., 2019). The displacements of the country rock layering similarly reflect a top-to-the SE deformation. Grantham et al., (1991) reported a Rb/Sr whole rock – mineral isochron of 469Ma ± 10Ma for the Dalmatian Granite. This age is supported by a SHRIMP U/Pb zircon age of 489Ma ± 5Ma by Krynauw and Jackson, (1996).

Discussion and Interpretation From the structures observed in Straumsnutane and their relative ages it can be interpreted that early top-to NW thrust faults, folds with a horizontal, NE-trending fold axis, and strong SE-dipping axial planar foliations, represent the oldest structures in Straumsnutane, i.e. D_1. The inference that some of these structures were syn-depositional in Straumsnutane would constrain the age of this deformation to ca. <1125Ma, as indicated by the

depositional age of the underlying Ahlmannrygen Group reported by Marschall *et al.,* (2013) and the age of the Borgmassivet suite of 1107 Ma (Hanson et al., 2006).

Steeply SE dipping foliation surfaces (S_1), NW-vergent thrusts with well-developed mylonites, and steeply SE-plunging stretching lineations suggest a D_1 paleostress ellipsoid with a gently NW-plunging σ_1, horizontal NE trending σ_2, and steeply SE plunging σ_3. Such a stress ellipsoid is similar to that suggested by the D_2 structures (Figure. 11, see below). However, the differences in vergence, between the interpreted D_1 structures (NW) and D_2 structures (WNW, ESE and E), and difference in the style of deformation (ductile D_1, exemplified by foliation and mylonitisation, cross cut by brittle/semi-brittle D_2, exemplified by slickensided fault surfaces and sigmiodal en-echelon vein arrays respectively), suggests the deformation recorded in the Straumsnutane area occurred in two separate events with D_1 top-to-NW and D_2 generally top-to-ESE.

Age constraints on the younger top-to-ESE structures (D_2) are provided by the K-Ar ages on syntectonic white mica of ~525Ma (Peters, 1989; Peters et al., 1990) from fault zones in Straumsnutane which were inferred to represent the age of shearing in late epidote quartz filled fault planes (Figure 11a). Support for this age of the timing of the younger deformation is provided by the broad lower intercept “age” of between 600-480Ma shown by discordant zircons reported by Marschall *et al.,* (2013) which were interpreted to result from low grade metamorphism recorded in the rocks.

The ca. 1100 Ma-age top-to NW D_1 deformation interpreted for Straumsnutane can be correlated with the $D_{1\text{-}2}$ deformation described by Grantham *et al.,* (1995) for the gneisses exposed in west Sverdrupfjella, where meta-granodoritic rocks with crystallisation ages of ~1140Ma (Grantham *et al.,* 2011) are reported. Low U metamorphic rims on the zircon grains similarly suggest a timing of

metamorphism between 514Ma and 660Ma (Grantham *et al.,* 2011). Early Neoproterozoic metamorphism in the Maud Province is inferred from migmatitic layering truncated by a metamorphosed mafic dyke with a poorly defined upper intercept age of ~950Ma (Grantham et al., 2006).

The ca. 525 Ma top-to ESE D_2 deformation recorded for Straumsnutane can be correlated with D_3 deformation described here in western Sverdrupfjella and reported by Grantham et al., (1995) and Grantham (1992). In western Sverdrupfjella, this deformation is expressed as SE-vergent asymmetric folds at Jutulrora, Brekkerista and Roerkulten (Grantham, 1992; Grantham et al., 2006) (Figures 14a and 14b) with granite vein emplacement in the dilation planes of deformation. These folds have a top-to-SE vergence similar to that described by Watters et al. (1991) in Straumsnutane as well as the folding reflected in Figure 7a.The folding (Figure 13d and Figure 15 e and f) and metamorphism of a mafic dyke at Roerkulten is consistent with top-to SE deformation and constrained by the lower intercept date of 523± 21 Ma (Grantham et al., 2006). Similarly, in eastern Sverdrpfjella, the syntectonic emplacement of the Dalmatian Granite at ~470-490 Ma is consistent with a top-to-SE brittle deformation event as indicated by SHRIMP U-Pb zircon data from the Dalmatian Granite indicating a crystallisation age of ~490Ma (Grantham et al., 1991; Krynauw and Jackson, 1996, Grantham et al., 2019). The age of metamorphism in western Sverdrupfjella is supported by a LA-ICPMS U/Pb age from titanite from Straumsvola (Figure 12) of 491 ± 27 Ma reported by Grosch et al., (2015).

It is significant to note that S to SE vergent structures and associated SE dipping granite sheets are limited to Sverdrupfjella and have not been reported in Kirwanveggan to the S (Grantham et al., 2019). Late D3 shearing of Pan African ca. 500 Ma age is inferred as having a top-to-SE sense of

shear in Heimefrontfjella however no syntectonic granite sheets have been recognised in Heimefrontfjella (Jacobs et al., 1996).

The structural characteristics for Sverdrupfjella described above and from Grantham *et al.,* (1995) have contributed to the interpretation of a mega-nappe structure (Grantham et al., 2008; Grantham et al., 2013; Grantham et al., 2019) resulting from the Kuunga Orogeny in which northern Gondwana (the EAO Namuno Terrane of N. Mozambique, Figures 2 and 16) was emplaced over southern Gondwana between ~550-500Ma, along a collision zone, between N. and S. Gondwana (Figure 2b). The timing of the Kuunga Orogeny, initially inferred as being 570-530 Ma by Meert (2003), is extended to younger ages of ca. 480 Ma, inferred from Ar-Ar data from Sverdrupfjella and Kirwanveggan (Grantham et al., 2019) as well as the emplacement of granite veins between ca. 520 - 490 Ma (Grantham et al., 2019). An integral part of the inferred nappe structure are the top-to SE D3 folds in western Sverdrupfjella (described here) in which these folds are seen as resulting from drag compressional structures in the footwall of the mega-nappe (Figure 16). Syntectonic emplacement of Dalmatian Granite at ca. 490Ma in both east and wst Sverdrupfjella with top-to-SE brittle structures in east Sverdrupfjella constrain the age of the deformation. The correlation of the similarly oriented top-to ESE D2 structures in Straumsnutane with D3 structures in Sverdrupfjella consequently suggests that the nappe structure probably traversed over the eastern edge of the Grunehogna Craton in NE Straumsnutane, as well as the Maud Belt, causing the top-to ESE structures recorded in eastern Straumsnutane and the west Sverdrupfjella Maud Belt. This interpretation is consistent with the low-grade metamorphic assemblages recorded in Straumsnutane and discordant zircons reported by Marschall et al., (2013). Pressure-temperature estimates of ~350^{o}C and 0.3-GPa on a metabasite assemblage on the eastern edge of Ahlmannryggen, south of Straumsnutane have been reported by Grosch et al., (2015) implying a burial depth of ca. 9km, consistent with the low grade minerals seen in the D_2

structures in Straumsnutane, and are consistent with burial and deformation beneath the nappe. No reliable thickness estimates for the Ritscherflya Supergroup in Antarctica are available, recognising the absence of continuous exposure in Antarctica and the difficulty of correlating sedimentary and volcanic units between nunataks. However, the Ritscherflya Supergroup is correlated with the Umkondo Group in southeastern Zimbabwe and central Mozambique (Hanson et al., 2006), which has an inferred thickness of ca. 3.7km (Bene, 2004). This would suggest that the metamorphic P-T estimates reported by Grosch et al., (2015) at ca. 500 Ma along the margin of the Grunehogna Craton, were probably the consequence of tectonic loading in the footwall, and cannot be ascribed solely to depositional burial.

In contrast, in NE Sverdrupfjella, the well constrained P-T path, reflecting isothermal decompression of ca. 1.4 GPa to ca. 0.6 GPa from ~570Ma to ~540Ma from NE Sverdrupfjella (Pauly et al., 2016) is consistent with a continent-continent collision setting in which eastern Sverdrupfjella and Gjelsvikfjella formed a hanging-wall block with ca. <598 Ma top-to-S and SSW thrusting (Jacobs et al., 2003; Baba et al., 2015). A doubly thickened crust in eastern Sverdrupfjella eastwards is supported by gravity studies (Riedel et al., 2012) which indicate crustal thicknesses >42 km over north eastern Sverdrupfjella, with P-T studies requiring significant erosion to expose high P-T assemblages at current levels.

The tectonic setting envisaged is comparable to that seen currently along the western edge of the setting involving India colliding with Eurasia, contributing to the Himalayan Orogeny (Figure 17a) with the Arabian Plate and India being subducted under Eurasia. Figure 17b shows a modified mirror image of Figure 17a, with appropriately named continental blocks inserted comprising the Kalahari Craton, Maud-Nampula Terranes (footwall) and East African Orogen-Cabo Delgardo Complex-Namuno Terrane (hanging wall). The broad deformation patterns involving tectonic

blocks on a similar scale in Mozambique extending into Antarctica, are similar to those seen in the Himalayan collision zone reflected in Figure 17a. Subsequent erosion of Mozambique and, to a lesser extent, Antarctica has exposed the geology as reflected in Figure 2, in which much of the nappe inferred here and in Grantham et al., (2008), Grantham et al., (2013) and Grantham et al., (2019) has been removed by erosion related to uplift, particularly over western Sverdrupfjella.

Conclusions

The deformation history of Straumsnutane involved D_1 top-NW thrust faulting and folding at ca. 1100 Ma with similarly oriented deformation of similar age being seen in west Sverdrupfjella to the east. D_1 deformation in Straumsnutane was followed by D_2 deformation comprising conjugate top-to the ESE and WNW deformation involving brittle-semi-ductile quartz veining, SE vergent folding and mesoscale faulting with the timing of this deformation constrained by low grade metamorphism at ~525 Ma. The deformation geometry of top-to-ESE and timing at ~525Ma is similar to that recorded for D_3 in Sverdrupfjella.

No evidence of sinistral displacement, consistent with a continent scale sinistral strike slip system, as inferred for the EAO, along the boundary between the Grunehogna Craton and the Maud Belt, interpreted by Perritt and Watkeys (2006) and Croaker (1999) have been seen in Straumsnutane or west Sverdrupfjella. In contrast the D_2 deformation in Straumsnutane and D3 in Sverdrupfjella are consistent with collisional structures with southward vergence. The D_3 deformation, metamorphism and intrusion of granites in Sverdrupfjella has been interpreted as resulting from the location of the area in the footwall of a south to SE emplaced mega-nappe structure (Grantham et al., 2008). The similarities in timing and style of deformation for D_2 in Straumsnutane with that of D_3 in Sverdrupfjella would suggest that the nappe structure was not restricted to the Maud and CDMLTerranes but also partially overlapped onto and was restricted to the eastern edge of the Grunehogna Craton in Straumsnutane with western Straumsnutane,

Ahlmanryggen and Borga areas showing no similar deformation. This conclusion is supported by the relatively high pressures of metamorphism along this margin, implying burial of ca. 9 km. Late (Pan African) D3 shearing in Heimefrontfjella similarly has a top-to-SE sense of shear (Jacobs (1996). Grantham et al., (2019) concluded that deformation along the eastern margin of the Grunehogna Craton did not affect southern Kirwanveggan and hence did not extend to Heimefrontfjella, the oblique strike-slip shearing in Heimefrontfjella, probably continuing northeastwards along the Forster Magnetic linearment to the Orvinfjella Shear zone in CDML. The deformation trajectories and related P-T conditions described here for ca. 525-480 Ma deformation in Straumsnutane and Sverdrupfjella, and associated melting in Sverdrupfjella as well as the published gravity data are consistent with the thickened crust mega-nappe model proposed for the Kuunga Orogeny in WDML sector of Antarctica. On a wider scale, a top-to-S low angle brittle shear zone with an age of <530 Ma has been described from Sor Rondane (Tsukada et al., 2017)(Figure 2). Similarly, the Kataragama Klippen in Sri Lanka, is interpreted as an erosional remnant of a top-to-S (in Gondwana framework) thrust nappe (Silva et al., 1981) (Figure 2) in which the Highlands Complex has been emplaced over the Vijayan Complex. This suggests the mega-nappe extended from the overlapping the Kalahari Craton in the west to Sri Lanka in the east with the Maud (W Sverdrpfjella), Barue and Nampula Complexes (N. Mozambique) and Vijayan Complex (Sri Lanka) representing footwall rocks to the nappe (Figure 2).

This tectonic setting is comparable to that along the western margin of the Tibetan plateau where India colliding northward with Asia is flanked on the west by a zone of sinistral transpressional orogeny extending through Pakistan and Afghanistan (Figure 17a).

Within the collisional setting envisioned in Figure 16, it could be expected that dextral, top-to-the SE displacement would occur between a footwall, comprising the Grunehogna craton plus western

Sverdrupfjella and hanging wall of eastern Sverdrupfjella plus Gjelsvikfjella and beyond. A degree of differential shear (dextral?) could be expected between the Grunehogna craton and Maud Belt, recognising the thicker more buoyant cratonic keel to the west and thinner metamorphic terrain to the east, as reflected in the gravity study of Riedel et al., (2012). Their study indicates crust >42km thick underlying the Grunehogna Craton and <38-40km underlying western Sverdrupfjella, increasing to >42 km over NE Sverdrupfjella and Gjelsvikfjella eastwards.

Acknowledgements

Research funding provided from the NRF via a SANAP grant (80267) and a personal grant to GHG (80915) is gratefully acknowledged. Logistical support from Department of Environmental Affairs is similarly acknowledged. Funding from CGS and the University of Pretoria is also most gratefully received. Constructive reviews by Horst Marschall and an anonymous reviewer are acknowledged.

Declaration of Interest

No conflict of interest is declared by the authors

References

Angelier, J. and Mechler,P. (1977) Sur une méthode graphique de recherece des contraintes principals également utilisable en tectoniqiue et en séismologie: la méthode des dièdres droits. *Bulletin de la Société Géologique de France* 7/19, 1309-1318.

Baba S., Owada M., and Shiraishi K. (2008) Contrasting metamorphic P-T path between Schirmacher Hills and Muhlig-Hoffman fjella, Central Dronning Maud Land, East Antarctica Geodynamic Evolution of East Antarctica:a Key to the East-West Gondwana Connection. eds M Satish-Kumar, Y Motoyoshi, Y Osanai, Y Hiroi and K Shiraishi, Geol. Soc. of London Spec. Publ., 308, 401-417.

Baba,S., Horie,K., Hokada, T., Owada, M., Adachi, T. and Shiraishi, K. (2015) Multiple Collisions in the East African–Antarctica Orogen: Constraints from Timing of Metamorphism in the Filchnerfjella and Hochlinfjellet Terranes in Central Dronning Maud Land. *The Journal of Geology*, 123, p. 55–78.

Bauer W., Thomas R.J., and Jacobs, J. (2003) Proterozoic-Cambrian history of Dronning Maud land in the context of Gondwana assembly. pp247-270 in *Proterozoic East Gondwana: Supercontinent Assembly and Breakup*. Yoshida M., Windley B.F. and Dasgupta S.(eds), Geol. Soc. Lond. Spec. Publ. 206, 247-265.

Bene, B.M. (2004) Tectonic evolution of western central Mozambique. (Unpubl PhD Thesis). University of Kwa-Zulu Natal, Durban, South Africa. 216pp.

Bingen, B. , Jacobs, J., Viola, G. , Henderson, I.H.C., Skår, Ø., Boyd, R., Thomas, R.J., Solli, A., Key R.M. and Daudi E.X.F. (2009) Geochronology of the Precambrian crust in the Mozambique belt in NE Mozambique, and implications for Gondwana assembly. *Precambrian Research*, 170, Pages 231-255.

Board W.S., Frimmel., H.E., & Armstrong R.A. (2005) Pan-African Tectonism in the western Maud Belt: P-T-t path for High-grade gneisses in the H.U. Sverdrupfjella, East Antarctica. *Journal of Petrology*, 46, 671-699.

Bons P.D., Elburg M.A. and Gomez-Rivas E. (2011) A review of the formation of tectonic veins and their microstructures. *Journal of Structural Geology*, 43, 33-62.

Byrnes G. (2015) *Tectono-metamorphic history of the reworked, high-grade Maud Belt at central-Eastern H.U. Sverdrupfjella, Antarctica*. unpubl. MSc thesis, University of Cape Town. pp. 126.

Cadoppi, P., Costa, M. and Sacchi, R. (1987) A cross section of the Namama Thrust belt (Mozambique). *Journal of African Earth Sciences*, 6, 493-504.

Croaker, M. (1999) *Geological constraints on the evolution of the Urfjell Group, southern Kirwanveggen, western Dronning Maud Land, Antarctica* .Unpubl. M.Sc. thesis, University of Natal. 160p.

Crupa W.E, Khana S.D., Huang J., Khan A.S., and Kasib A. (2017) Active tectonic deformation of the western Indian plate boundary: A case study from the Chaman Fault System. *Journal of Asian Earth Sciences*, 147., 452-468.

Daszinnies, M. C., Jacobs, J., Wartho J-A., and Grantham G.H. (2009) Post Pan-African thermo-tectonic evolution of the north Mozambican basement and its implication for the Gondwana rifting. Inferences from 40Ar/39Ar hornblende, biotite and titanite fission-track dating. *Geological Society of London, Special Publications* 2009; v. 324; p. 261-286.

Eastin R., Faure G. and Neethling D.C. (1970) The age of the Trollkjellrygg Volcanics of western Queen Maud Land. *Antarctic Journal, 5*, 157-158.

Fitzsimons,I.C.W. (2000). Grenville-age basement provinces in east Antarctica: evidence for three separate collisional orogens. *Geology*, 28, 879-882.

Grantham, G.H. (1992) *Geological Evolution of western H.U. Sverdrupfjella, Dronning Maud Land, Antarctica.* Unpublished PhD thesis, University of Natal (Pietermaritzburg). 277pp.

Grantham, G.H. (1996) Aspects of Jurassic Magmatism and Faulting in western Dronning Maud Land, Antarctica: Implications for Gondwana breakup pp 63-71 in *Weddell Sea Tectonics and Gondwana Break-up*. Storey, B.C., King, E.C. and Livermore, R.A. (Eds). Geological Society of London Special Publication No. 108.

Grantham, G.H., Armstrong. R.A. and Moyes, A.B. (2006) The age, chemistry and structure of mafic dykes at Roerkulten, H.U. Sverdrupfjella, western Dronning Maud Land, Antarctica. pp.213-224 in *Dyke Swarms - Time Markers of Crustal Evolution.* Hanski E., Mertanen S. Ramo T. and Vuollo J. (eds) Proceedings of the Fifth/Fourth International Dyke Conference (IDC5), Rovaniemi, Finland. A.A. Balkema Press.

Grantham, G.H., Jackson, C., Moyes, A.B., Groenewald, P.B., Harris, P.D., Ferrar, G. & Krynauw, J.R., (1995) The tectonothermal evolution of the Kirwanveggan-H.U. Sverdrupfjella areas, Dronning Maud Land, Antarctica. *Precambrian Research*, 75, 209-230.

Grantham G.H, Kramers J., Eglington, B and Burger E.P. (2019). The Ediacarian-Cambrian tectonic evolution of western Dronning Maud Land : New ^{40}Ar-^{39}Ar and Sr/Nd data from Sverdrupfjella and Kirwanveggan, the source of the Urfjell Group and Implications for the Kuunga Orogeny and Gondwana amalgamation . *Precambrian Research*. https://doi.org/10.1016/j.precamres.2019.105444.

Grantham, G.H., Maboko, M. and Eglington, B.M. (2003) A review of the evolution of the Mozambique Belt and implications for the amalgamation of Rodinia and Gondwana. pp 401 - 426 in *Proterozoic East Gondwana: Supercontinent Assembly and Breakup*. Yoshida M., Windley B.F. and Dasgupta S.(eds), Geological Society of London Special Publication 206.

Grantham, G.H, Macey,P.H., Ingram, B.A., Roberts, M.P, Armstrong R.A., Hokada T., Shiraishi, K., Jackson C., Bisnath, A., Manhica V. (2008) Terrane Correlation between Antarctica, Mozambique & Sri Lanka; Comparisons of Geochronology, Lithology, Structure and Metamorphism and possible implications for the geology of southern Africa and Antarctica. in *Geodynamic Evolution of East Antarctica:a Key to the East-West Gondwana Connection.* eds M Satish-Kumar, Y Motoyoshi, Y Osanai, Y Hiroi and K Shiraishi, Geol. Soc. of London Spec. Publ., 308, p91-119.

Grantham G.H., Manhica A.D.S.T., Armstrong, R.A., Kruger, F.J. and Loubser M. (2011) New SHRIMP, Rb/Sr and Sm/Nd isotope and whole rock chemical data from central Mozambique and western Dronning Maud Land, Antarctica: implications for the nature of the eastern margin of the Kalahari Craton and the amalgamationof Gondwana. *Journal of African Earth Sciences* 59, 74–100.

Grantham, G.H., Moyes, A.B. and Hunter, D.R. (1991) The age, petrogenesis and emplacement of the Dalmatian Granite, H.U. Sverdrupfjella, Dronning Maud Land, Antarctica. *Antarctic Science*, 3, 197-204.

Grantham, G.H., Storey B.C., Thomas R.J., Jacobs J. (1997) The pre-breakup position of Haag Nunataks within Gondwana: possible correlatives in Natal and Dronning Maud Land. *The Antarctic Region: Geological Evolution and pro*cesses. Ed C.A. Ricci. Proc. VII Int. Symposium on Antarctic Earth Sciences, Siena, 13-20. Terra Antarctica.

Groenewald, P.B. and Hunter, D.R. (1991) Granulites of northern H.U. Sverdrupfjella, western Dronning Maud land: metamorphic history from garnet-pyroxene assemblages, coronas and hydration reactions. pps 61-67 in *Geological evolution of Antarctica*. Thomson, M.R.A., Crame, J.A. and Thomson, JW. (eds). International Symposium on Antarctic Earth Sciences, Cambridge.

Grosch, E.G., Bisnath, A., Frimmel H.E.and Board W.S. (2007) Geochemistry and tectonic setting of mafic rocks in western Dronning Maud Land, East Antarctica: implications for the geodynamic evolution of the Proterozoic Maud Belt. *Journal of the Geological Society, London*, Vol. 164, 2007, pp. 465–475.

Grosch E.G. , Frimmel H.E., Abu-Alam Tamer & Košler J. (2015) Metamorphic and age constraints on crustal reworking in the western H.U. Sverdrupfjella: implications for the evolution of western Dronning Maud Land, Antarctica. *Journal of the Geological Society of London*, 172, 499-518.

Grunow A., Hanson R and Wilson T. (1996) Were aspects of Pan-African deformation linked to Iapetus opening? *Geology*, 24, 1063-1066.

Hanson R.E, Harmer R.E., Blenkinsop T.G.,Bullen D.S, Dalziel I.W.D.,Gose W.A, Hall R.P., Kampunzu A.B.,Key R.M., Mukwakwami J.,Munyanyiwa H., Pancake J.A., Seidel E.K. and Ward S.E.

(2006) Mesoproterozoic intraplate magmatism in the Kalahari Craton: A review. *Journal of African Earth Sciences,* 46,141–167.

Harris C. and Grantham, G.H. (1993) Geology and petrogenesis of the Straumsvola nepheline syenite complex, Dronning Maud Land, Antarctica. *Geological Magazine*, 130, 513-532.

Harris C., Watters, B.R. and Groenewald, P.B. (1991) Geochemistry of the Mesozoic regional basic dykes of western Dronning Maud land, Antarctica. *Contributions to Mineralogy and Petrology*, 107, 100-111.

Jacobs, J. Ahrendt, H., Kreutzer, H. and Weber, K. (1995) K-Ar, 40Ar/39Ar and apatite fission-track evidence for Neoproterozoic and Mesozoic basement rejuvenation events in the Heimefrontfjella and Mannefallknausane (East Antarctica). *Precambrian Research,* 75, 251-262.

Jacobs J. and Thomas R.J. (2004) Himalayan-type indenter-escape tectonics model for the southern part of the late Neoproterozoic–early Paleozoic East African–Antarctic orogen. *Geology*, 32; p. 721–724.

Jacobs, J. Bauer, W., Spaeth, G., Thomas, R.J. and Weber, K. (1996) Lithology and structure of the Grenville-aged (~1.1Ga) basement of Heimefrontfjella. Geologische Rundschau, 85, 800-821.

Jacobs, J. Bauer W. Fanning C.M. (2003a) New age constraints for Grenvilian age metamorphism in western central Dronning Maud Land (East Antarctica) and implications for the paleogeography of Kalahari in Rodinia. *Geologische Rundschau*, 92, 301-315

Jacobs, J. Bauer W. Fanning C.M. (2003b) Late Neoproterozoic/Early Paleozoic events in central Dronning Maud Land and significance for the southern extension of the East African Orogen into East Antarctica. *Precambrian Research* 126, 27-53.

Jacobs J., Bingen, B., Thomas, R.J., Bauer, W., Wingate M.T.D. and Feitio P. (2008) Early Palaeozoic orogenic collapse and voluminous late-tectonic magmatism in Dronning Maud

Land and Mozambique: insights into the partially delaminated orogenic root of the East African-Antarctic Orogen? Geological Society of London Special Publication, v. 308; p. 69-90.

Jacobs, J. Fanning C.M., Henjes-Kunst F., Olesch M., and Paech H.J. (1998) Continuation of the Mozambique Belt into East Antarctica: Grenville age metamorphism and Polyphase Pan-African high grade events in Central Dronning Maud Land. *Journal of Geology*, 106, 385-406.

Jacobs, J. Falter M., Weber K. and Jessberger E.K. (1997) 40Ar/39Ar Evidence for the Structural Evolution of the Heimefront Shear Zone (western Dronning Maud Land) East Antarctica. pp 37-44 In *The Antarctic Region: Geological Evolution and processes*. Ed C.A. Ricci. Proc. VII Int. Symposium on Antarctic Earth Sciences, Siena, 13-20. Terra Antarctica.

Jacobs, J. Hansen, B.T., Henjes-Kunst, F., Thomas, R.J., Weber, K., Bauer, W., Armstrong, R.A. and Cornell, D.H. (1999) New Age constraints on the Proterozoic/Lower Paleozoic Evolution of Heimefrontfjella, East Antarctica, and its bearing on Rodinia/Gondwana Correlations. *Terra Antartica*, 6(4), 377-389.

Jacobs, J. Klemd R., Fanning C.M. Bauer W. & Colombo F. (2003c) Extensional collapse of the late Neoproterozoic-early Paleozoic East African-Antarctic Orogen in Central Dronning Maud Land, East Antarctica. pp271-287 in *Proterozoic East Gondwana: Supercontinent Assembly and Breakup*. Yoshida M., Windley B.F. and Dasgupta S.(eds), Geological Society of London Special Publication ,206.

Krynauw, J.R. and C. Jackson. (1996) Geological evolution of western Dronning Maud Land within a Gondwana framework. South African National Antarctic Programme Final Report 1991-1996. Geology Subsection , 1-48.

Macey P.H., Miller J.A., Rowe C.D. Grantham G.H., Siegfried P., Armstrong R.A., Kemp J. and Bacalau J. (2013) Geology of the Monapo Klippe, NE Mozambique and its significance for

assembly of central Gondwana. *Precambrian Research* doi.org/10.1016/j.precamres.2013.03.012

Macey, P.H. Thomas, R.J. Grantham, G.H.Ingram, B.A. Jacobs, J., Armstrong, R.A., Roberts, M.P. Bingen, B. Hollick, L. de Kock,G.S. Viola,G. Bauer, W. Gonzales, E. Bjerkgård, T., Henderson, I.H.C. Sandstad, J.S. Cronwright, M.S. Harley, S.Solli, A. Nordgulen, Ø. Motuza, G. Daudi E. and Manhiça V. (2010) Mesoproterozoic geology of the Nampula Block, northern Mozambique: Tracing fragments of Mesoproterozoic crust in the heart of Gondwana *Precambrian Research*, 182, p 124-148.

Marschall, H.R.,. Hawkesworth, C.J. and Leat P.T. (2013) Mesoproterozoic subduction under the eastern edge of the Kalahari-Grunehogna Craton preceding Rodinia assembly: The Ritscherflya detrital zircon record, Ahlmannryggen, Dronning Maud Land, Antarctica. *Precambrian Research* 236 (2013) 31– 45.

Marschall, H.R., Hawkesworth, C.J., Storey, C.D., Dhuime, B., Leat, P.T., Meyer, H-P., Tamm-Buckle, S., (2010). The Annandagstoppane granite, East Antarctica: evidence for Archaean intracrustal recycling in the Kaapvaal-Grunehogna craton from zircon O and Hf isotopes. *Journal of Petrology* 51, 2277–2301.

Meert J. (2003) A synopsis of events related to the assembly of eastern Gondwana. *Tectonophysics*, 362, 1-40.

Mendonidis P., Thomas R.J., Grantham G.H., Armstrong R.A. (2015) Geochronology of emplacement and charnockite formation of the Margate Granite Suite, Natal Metamorphic Province, South Africa:Implications for Natal-Maud belt correlations. *Precambrian Research*,265, 198-202.

Mieth M. and Jokat W. (2014) New aeromagnetic view of the geological fabric of southern Dronning Maud Land and Coats Land,East Antarctica. *Gondwana Research,* 25, 358–367.

Moabi N.G, Grantham G.H.,Roberts J., and le Roux P. (2017) The geology and geochemistry of the Straumsnutane Formation, Straumsnutane, western Dronning Maud Land, Antarctica and its tectonic setting on the western margin of the Kalahari Craton: additional evidence linking it to the Umkondo Large Igneous Province. In Pant, N. C. & Dasgupta, S. (eds) *Crustal Evolution of India and Antarctica: The Supercontinent Connection.* Geological Society, London, Special Publications, 457, https://doi.org/10.1144/SP457.4.

Pauly J., Marschall H.R., Meyer H-P., Chatterjee, N. and Brian Monteleone B. (2016) Prolonged Ediacaran–Cambrian Metamorphic History and Short-lived High-pressure Granulite facies Metamorphism in the H.U. Sverdrupfjella, Dronning Maud Land (East Antarctica): Evidence for Continental Collision during Gondwana Assembly. *Journal of Petrology*, 2016, Vol. 57, 185–228.

Perrit S.H. and Watkeys M.K. (2003) Implications of late Pan-African shearing in western Dronning Maud Land, Antarctica. pp135-143 in *Intraplate strike-slip deformation belts*. Storti F., Holdsworth R.E. and Salvini F (eds) . Geological Society of London Special Publication. 210.

Peters M., (1989) Igneous rocks in western and central Neuschwabenland, Vestfjella and Ahlmannryggen, Antarctica: petrography, geochemistry, geochronology, paleomagnetism, geotectonic implications. *Beri. Polarforschung* 61, 78–80.

Peters M., Haverkamp B., Emmermann R., Kohnen H. and Weber K. (1990) Paleomagnetism, K-Ar dating and geodynamic setting of igneous rocks in western and central Neuschwabenland, Antarctica. *In Geological Evolution of Antarctica.* Thompson M.R.A., Crame JA. and Thompson, JW. (eds) Proceedings of 5th ISAES, Cambridge. Cambridge University Press. 549-555.

Ramsay, J.G. (1967) *Folding and Fracturing of Rocks*. McGraw-Hill Book Co., New York, 568pps.

Riedel S., Jokat, W. and Steinhage D. (2012) Mapping tectonic provinces with airborne gravity and radar data in Dronning Maud Land, East Antarctica. *Geophysical Journal International*, 189, 414–427.

Riley T.R., Leat P.T., Curtis M.L., Millar I.L. Duncan R.A. and Fazel A. (2005) Early-Middle Jurrassic dolerite dykes from western Dronning Maud land (Antarctica): Identifying Mantle sources in the Karoo Large Igneous province. *Journal of Petrology*,46,1489-1524.

Rose K.C., Ferraccioli F., Jamieson S.J.R, Bell R.E., Corr H., Creyts T., Braaten T., Jordan T.A., Fretwell P.T., and Damaske D. (2013) Early East Antarctic Ice Sheet growth recorded in the landscapeof the Gamburtsev Subglacial Mountains. *Earth and Planetary Science Letters*, 375, 1-12.

Shackleton R.M. (1996) The final collision between East and West Gondwana: where is it? *Journal of African Earth Sciences,* 23, 271-287.

Silva,K.P.L., Wimalasena, E.M., Sarathchandra, M.J., Munasinghe,T., Dasannayake, C.B. (1981) The geology and origin of the Kataragama Complex of Sri Lanka. *Journal of the National Science Council of Sri Lanka*, 9(2), 189-197.

Spaeth, G. (1987) Aspects of the structural evolution and magmatism in western New Schabenland, Antarctica. pps 295-307 In *Gondwana Six: Structure, Tectonics and Geophysics*. G.D. McKenzie (ed). American Geophysical Union, Washington D.C. 323pps.

Spaeth, G. and Fielitz, W. (1987) Structural investigations in the Precambrian of western Neuschwabenland, Antarctica. *Polarforsching,* 57, 71-92.

Stern R.J. (1994) Arc assembly and continental collision in the Neoproterozoic East African Orogen: Implications for the consoildation of Gondwanaland. *Annual Reviews Earth Science*, 22, 319-351.

Stern R.J. (2002) Crustal evolution in the East African Orogen: a neodymium isotopic perspective *Journal of African Earth Sciences*, 34, 109-117.

Tsukada, K., Yuhara, M., Owada, M., Shimura, T., Kamei, A., Kouchi, Y. and Yamamoto K. (2017) A low-angle brittle shear zone in the western Sør Rondane Mountains, Dronning Maud Land, East Antarctica — Implication for assembly of Gondwanaland. *Journal of Geodynamics*, 111 ,15–30.

Wai-Pan Ng, S., Whitehouse M.J. Tama, T.P., Jayasingha P., Wonga, J.P., Denyszyn S.W., Yiu J.S. and Chang S-C. (2017) Ca. 820–640 Ma SIMS U-Pb age signal in the peripheral Vijayan Complex, Sri Lanka: Identifying magmatic pulses in the assembly of Gondwana. Precambrian Research, 294, 244-256.

Watters B.R., Krynauw J.R and Hunter D.R. (1991) Volcanic rocks of the Proterozoic Jutulstraumen Group in western Dronning Maud Land, Antarctica. pp41-46 in *Geological Evolution of Antarctica.* pps 41-46 in Geological evolution of Antarctica. Thomson, M.R.A., Crame, JA. and Thomson, JW. (eds). Cambridge University Press, Cambridge.

Watters, B.R. (1972) The Straumsnutane Volcanics, western Dronning Maud Land, Antarctica. *South African Journal Antarctic Research*, 2, 23-31.

Wilson T.J., Grunow A.M. and Hanson R.E. (1997) Gondwana assembly: the view from southern Africa and East Gondwana. *Journal of Geodyn*amics, 23, 263-268.

Wolmarans, L.G. and Kent, L.E. (1982) Geological investigations in western Dronning Maud Land, Antarctica - a synthesis. *South African Journal of Antarctic Research*, 93pps.

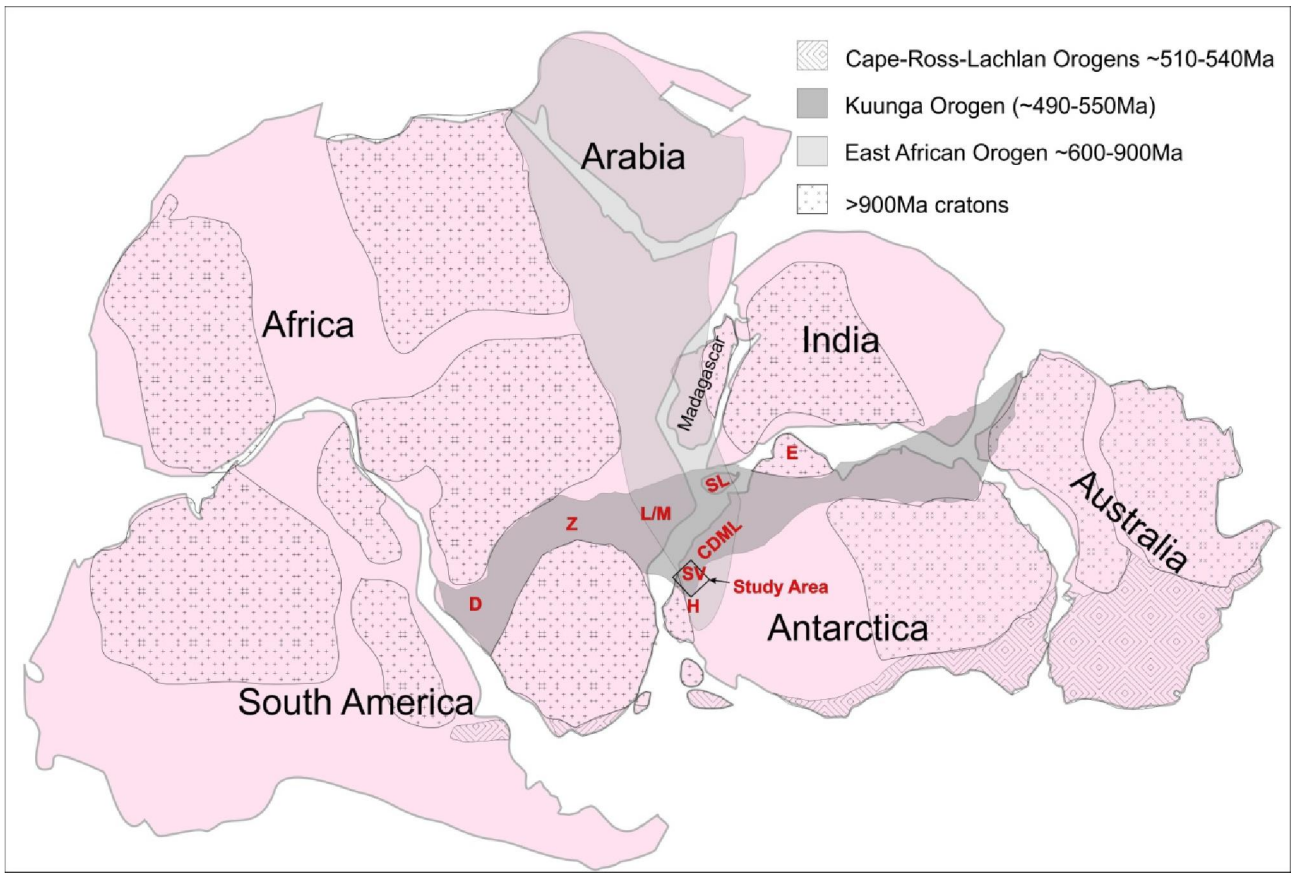

Figure 1. Reconstruction of Gondwana showing the location of the study area in a locality within the inferred extents of the East African Orogeny and the Kuunga Orogeny. D= Damara, Namibia; Z=Zambesi, Zambia; M/L=Mozambique/Lurio Belts, Mozambique; SL=Sri Lanka, E=Enderby Land, Antarctica; H=Heimefrontfjella, Antarctica.

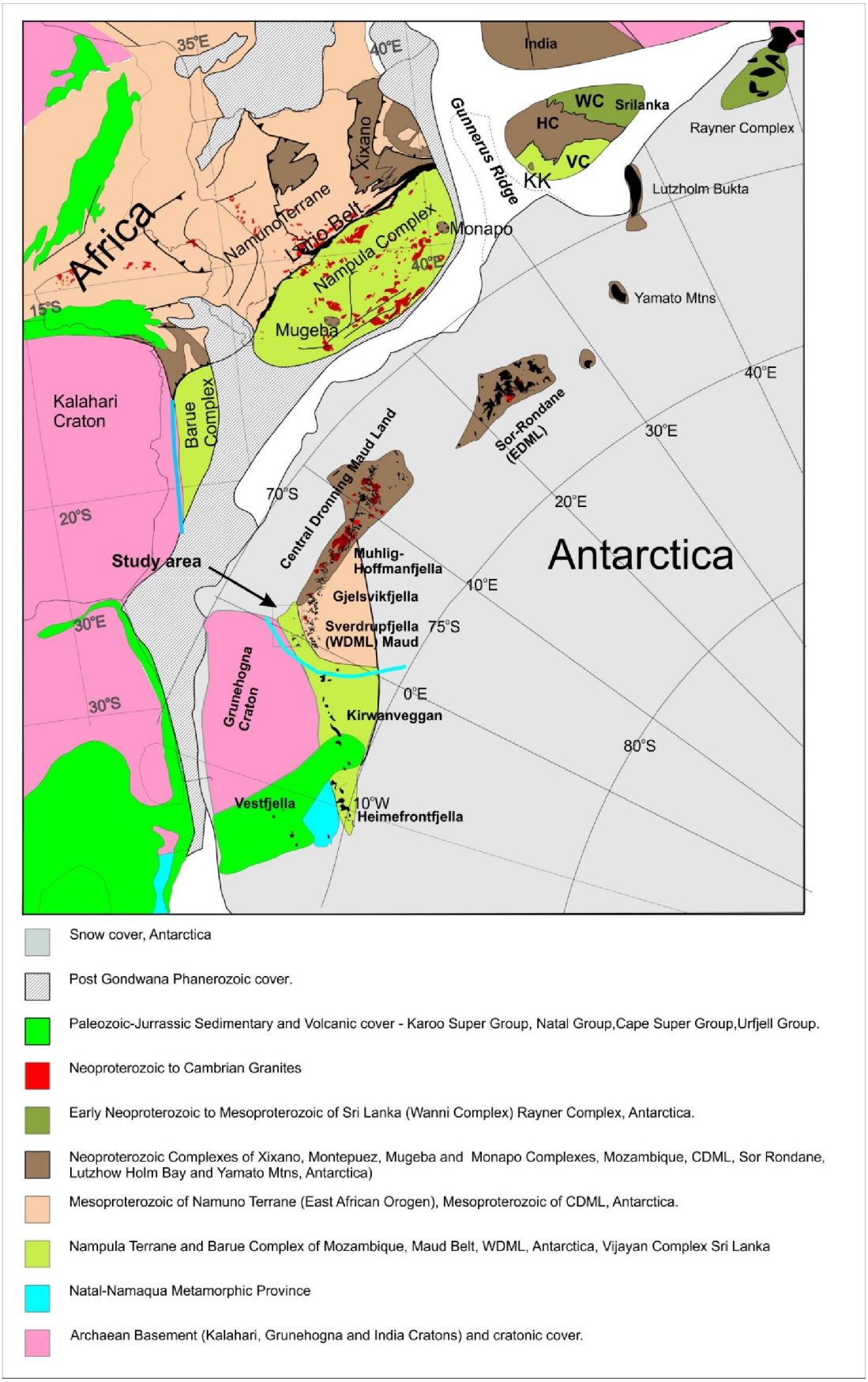

Figure 2. Simplified geological map of a portion reconstructed Gondwana showing correlated units between the different continental blocks. The study area location is shown along the boundary of the Kalahari Craton and Maud Belt. Abbreviations for Sri Lanka are WC=Wanni Complex, HC=Highlands Complex, VC=Vijayana Complex and KK=Kataragama Klippen. The blue line reflects the nappe extent inferred in this study.

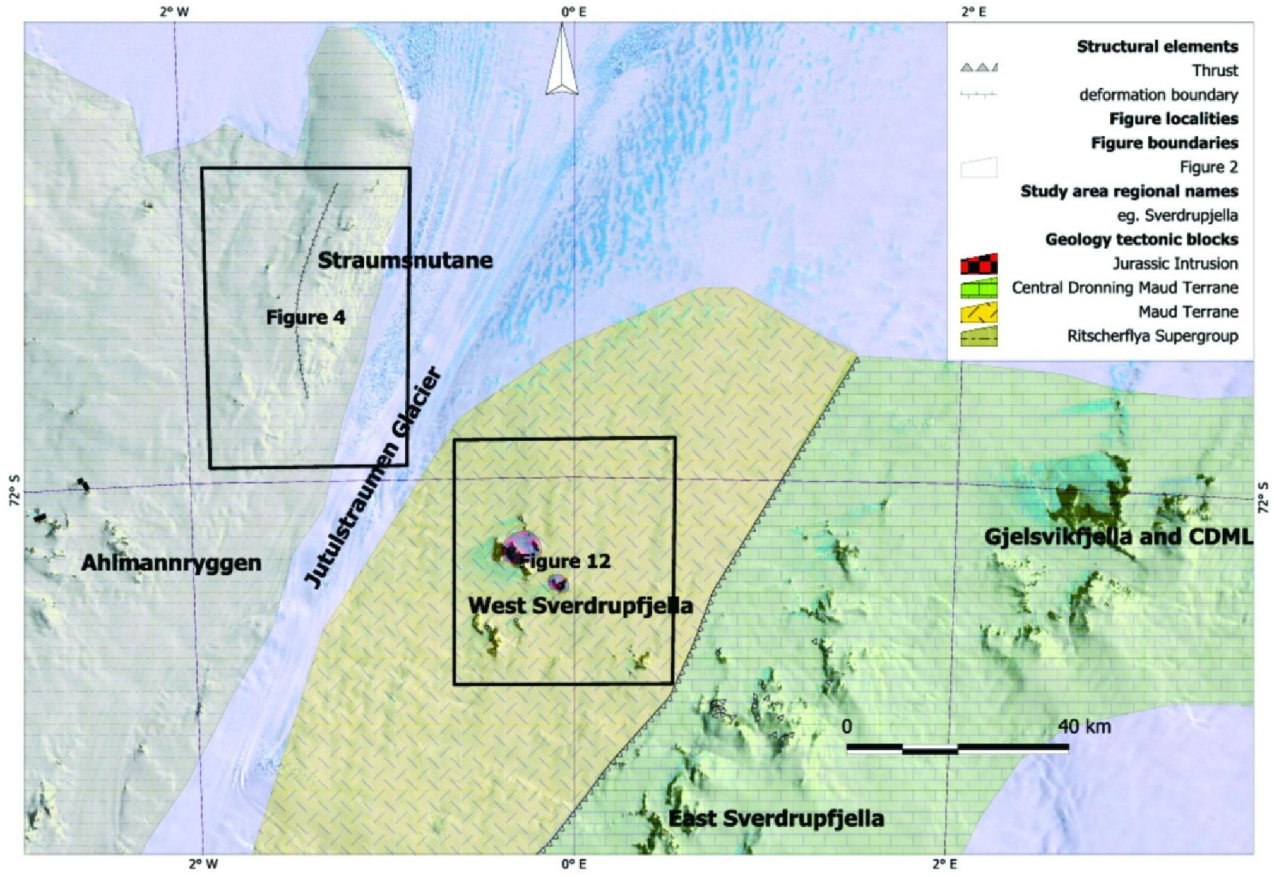

Figure 3. Map showing the location of the study area in western Dronning Maud Land, Antarctica, spanning the Jutulstraumen Glacier, the geological provinces and localities of maps in Figures 4 and 12 in western Dronning Maud Land. Note the inferred thrust fault boundary inferred between east and west Sverdrupfjella after (Grosch et al., 2015, Grantham et al., 2019) separating the Maud Belt from CDML terrane.

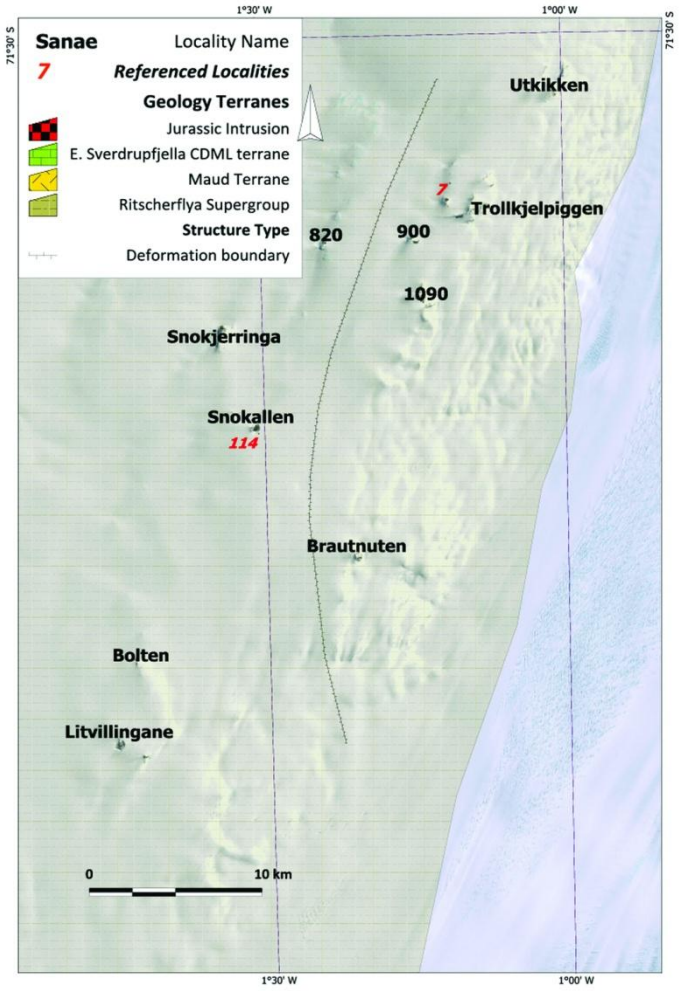

Figure 4. Map showing the nunataks where the Straumsnutane Formation is exposed in western Dronning Maud Land and the names of the various nunataks mentioned as well as locality numbers described in the text. The map also shows a dividing line between strongly deformed nunataks in the east and weakly deformed nunataks in the west.

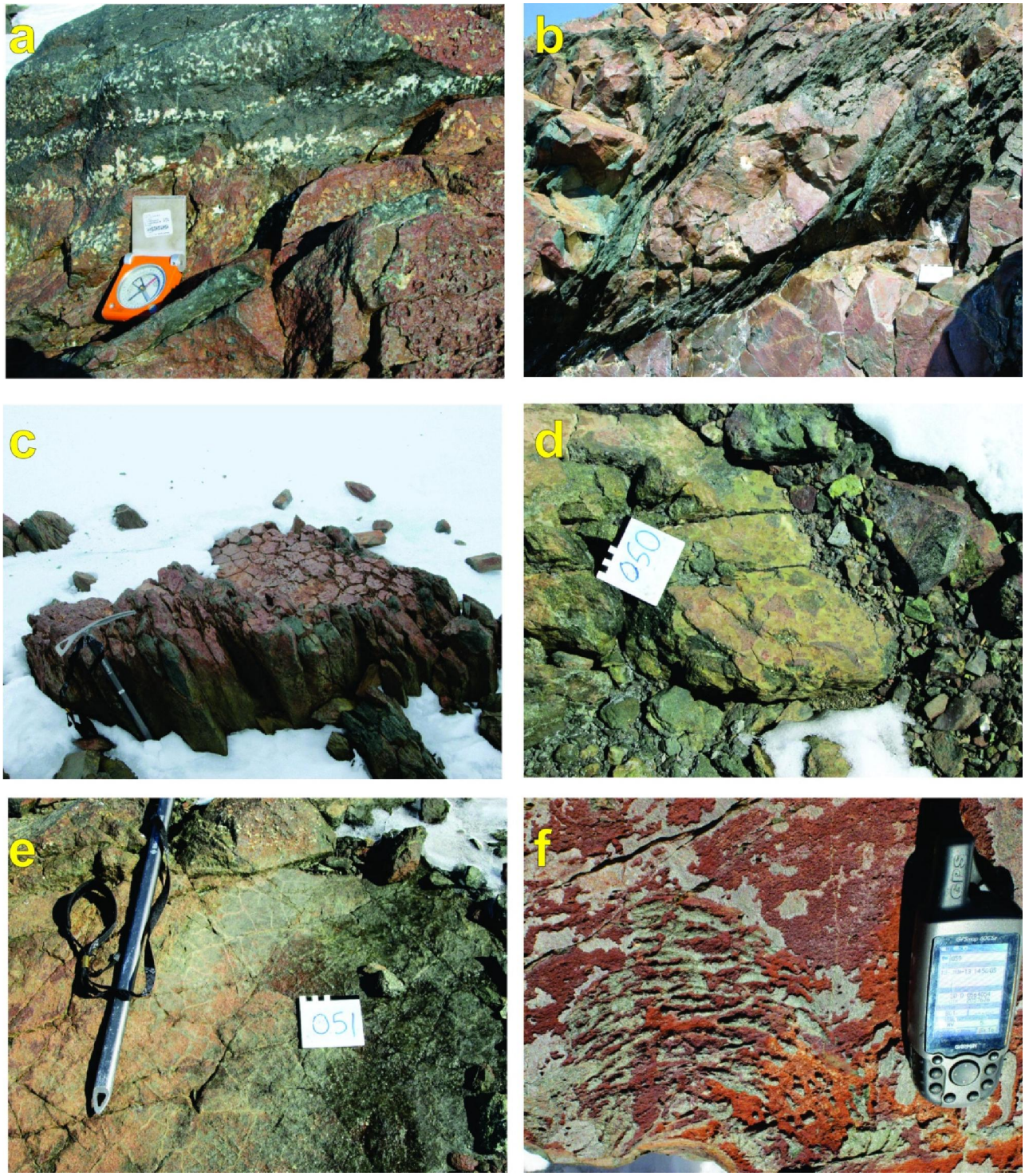

Figure 5. Photographs of primary structures recorded in the Straumsnutane area. Primary structures are best preserved in the western nunataks with deformation increasing toward the Jutulstraumen Glacier in the east. (a) layers rich and poor in amygdales. Compass for scale. (b) Flattened pillow lava. Note the strong planar fabric in the inter-pillow material and the unfoliated pillow core. The white square at lower right is 10cm wide. (c) Partially flattened columnar jointing in basaltic andesite. Ice axe for scale. (d) Volcanic breccia fragments in basaltic andesite. The white square is 10cm wide (e) Cooling cracks developed in basaltic andesite. Ice axe for scale (f) Surface pahoehoe ropy lava texture developed on basaltic andesite. GPS for scale.

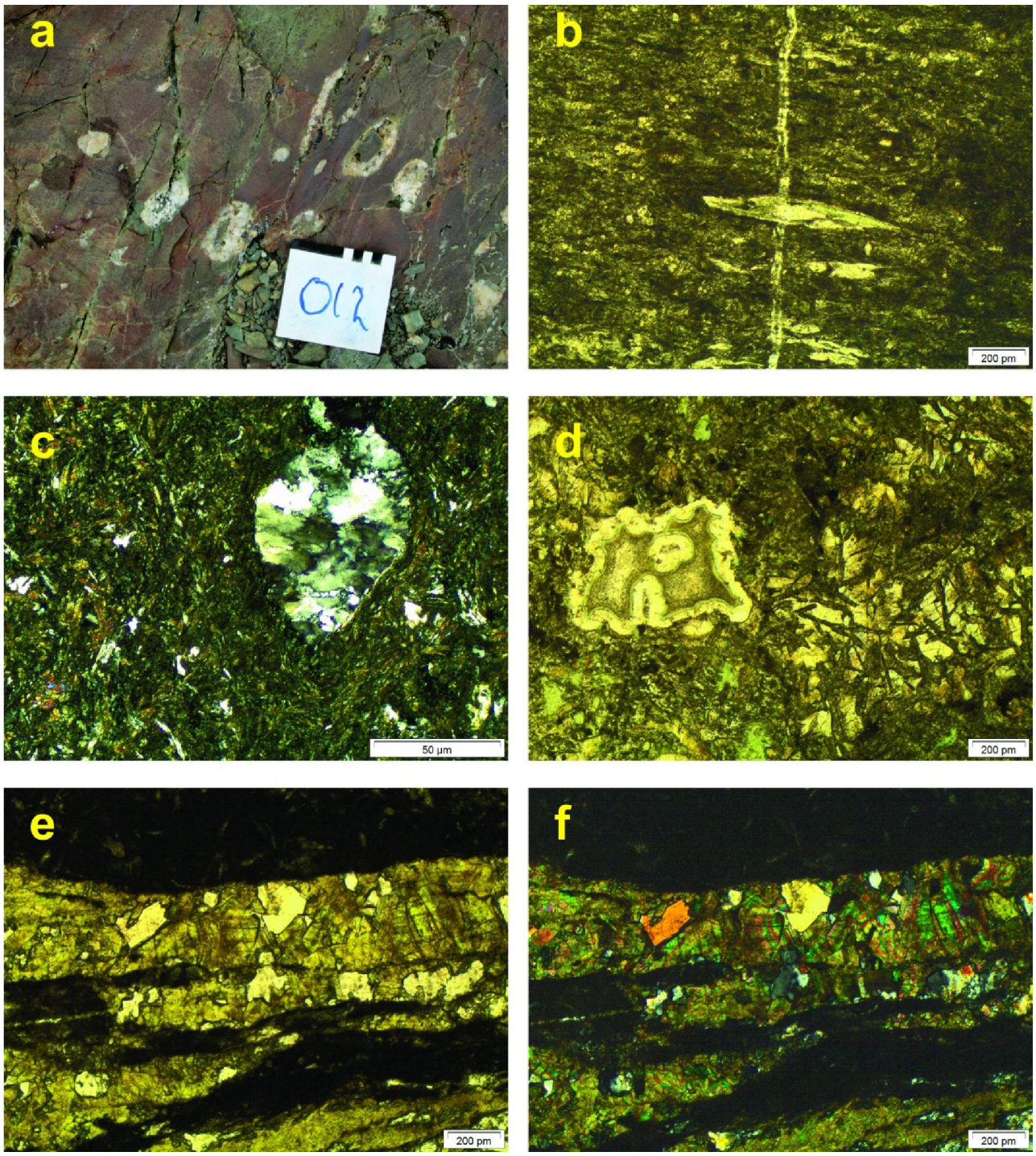

Figure 6. Field photograph and photomicrographs of thin sections. (A) Field photograph showing lenticular quartz tubes/blobs with cores of lavas. White square is 10cm wide. (B) Photomicrograph of mylonitic fabric and quartz vein in sheared basaltic andesite (C) Photomicrograph of amygdale in basaltic andesite showing strained quartz filling the amygdale. (D) Photomicrograph of zeolite filled amygdale at left in lava with partially altered clinopyroxene at right and green chlorite at bottom centre. (E) Photomicrograph (plane polarised light) of epidote quartz vein showing prismatic epidote. (F) Photomicrograph (crossed polars) of quartz epidote filled vein.

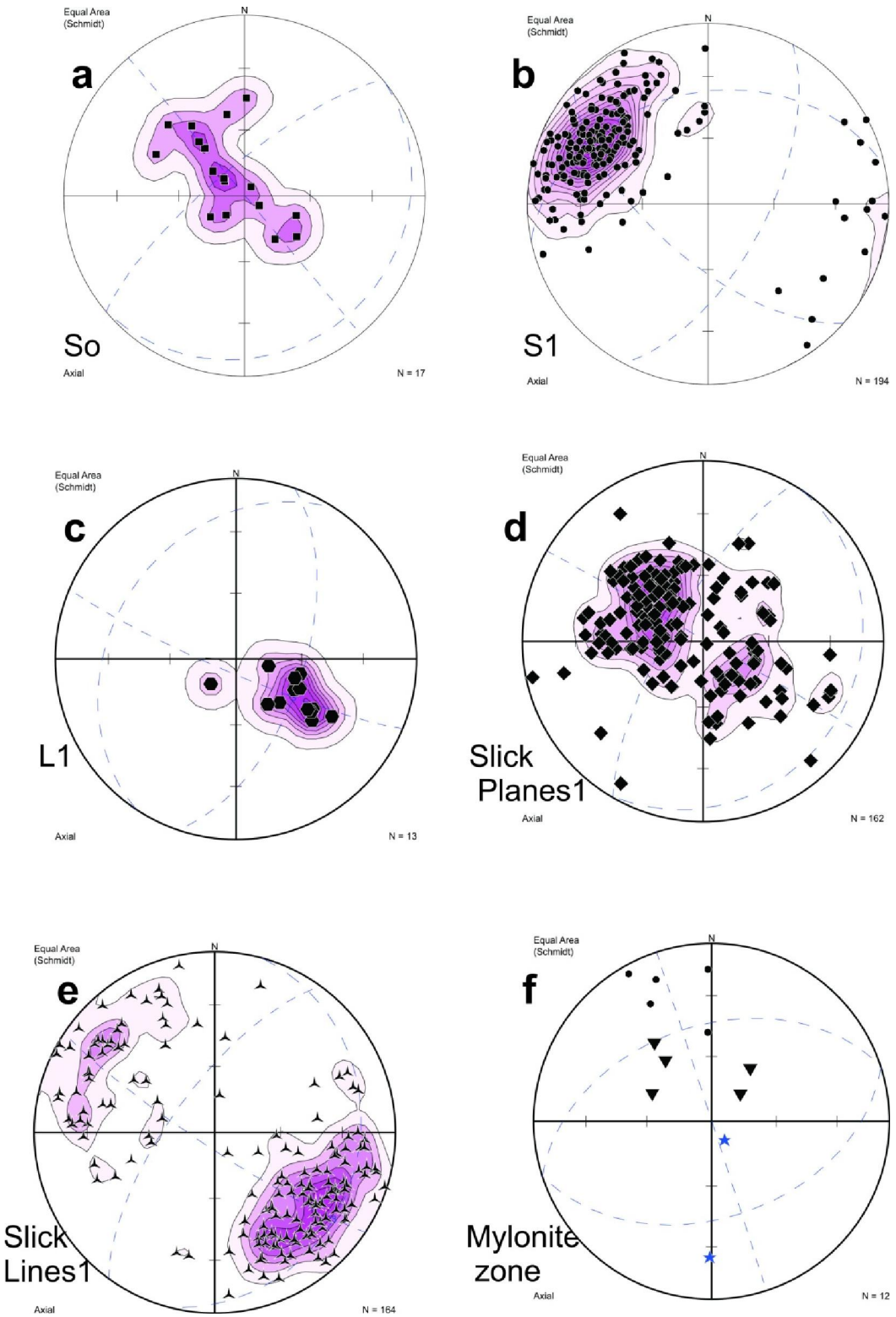

Figure 7. Contoured stereographic projections of (a) poles to primary layering from Snokjerringa defining gentle open folding with NE/SW oriented fold axis (b) poles to planar S_1 fabrics from the strongly sheared lavas in the west (c) mineral and stretching lineations (d) poles to slickensided fault surfaces (e) lineation directions from slickensided fault surfaces (f) structural data from the mylonite exposure described in Figure 8. Small dots are poles to planar fabrics in the country rock, inverted triangles are poles to mylonitic layering and stars are lineations in the mylonite and thrust fault splay plane.

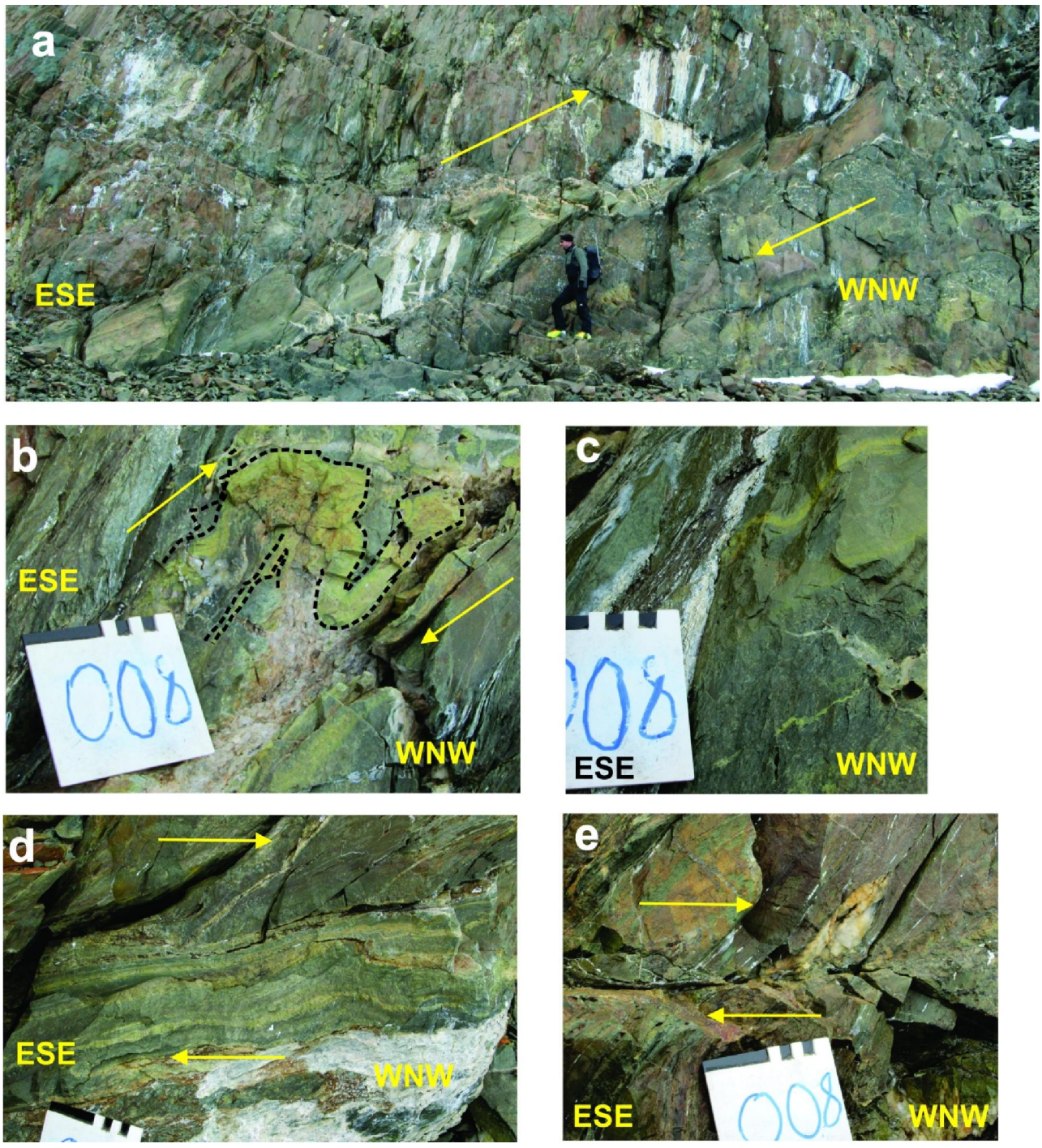

Figure 8. Photographs of structures recorded in Straumsnutane at locality 7 (Figure 4). (a) View facing southwards showing a 1-2m thick ultramylonitic layer, inclined from top right to bottom left, at south-western Trollkjellpiggen. Person at lower centre for scale. The structures suggest a top-to-NW sense of shear. (b) Detailed annotated photograph showing a flow fold within the mylonitic layer defined by a pale-green epidote rich layer showing a top to the NW sense of movement. (c) Photograph of truncation of an epidote rich layer by younger ramp structure. Note the folded quartz vein at lower right. (d) Photograph of the angular contact between the ultramylonite layer (below) and the foliated basaltic andesite above showing a top-to-NW shear sense. (e) Photograph of a truncated quartz lens by a thrust fault splay off the mylonite ultramylonite layer above showing a top-to-NW shear sense.

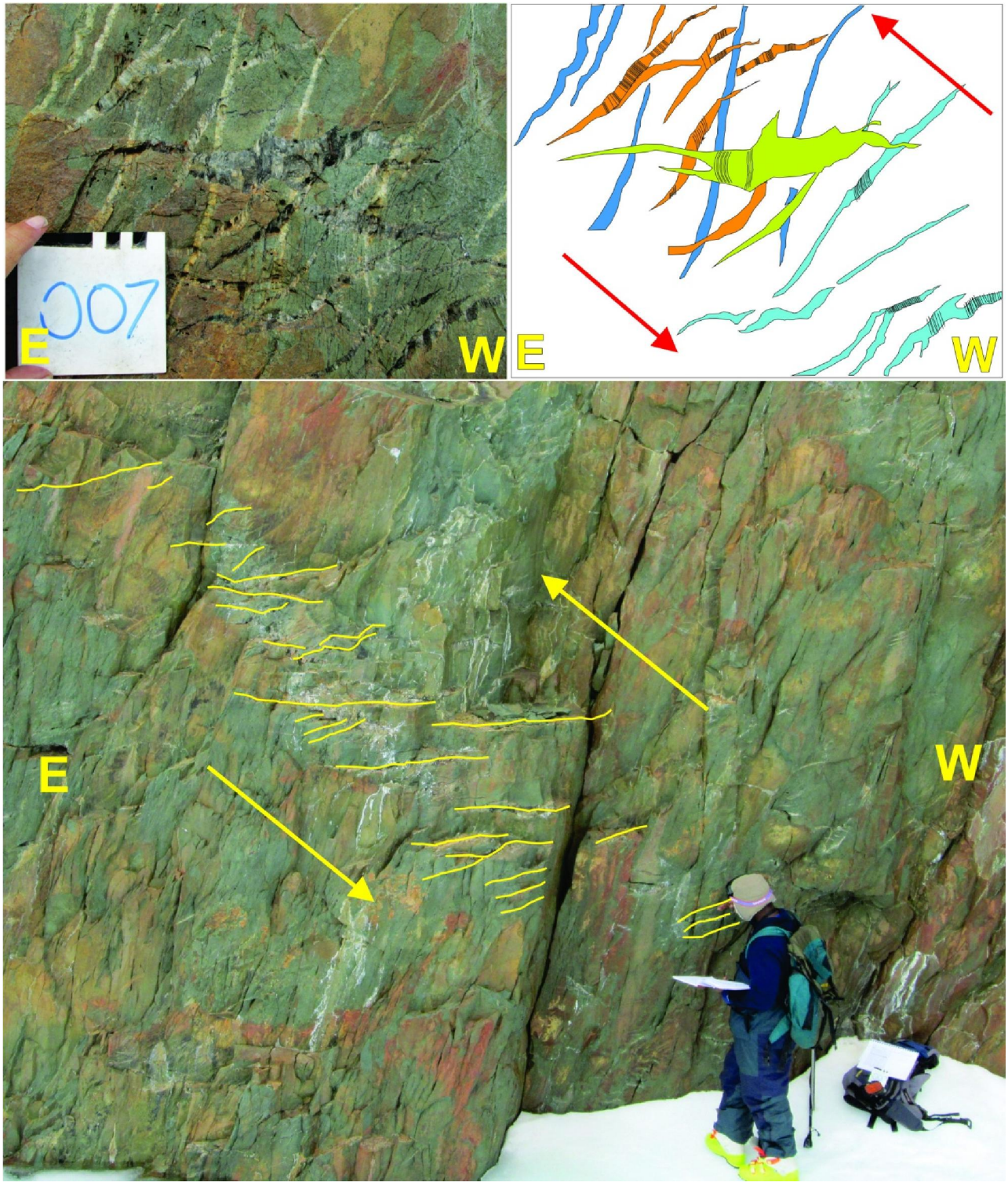

Figure 9. Photographs of structures recorded in the Straumsnutane area at locality 7 (Figure 4). (bottom) En-echelon quartz vein array in the edge of a wind scoop (person for scale). (top left) Photograph showing different generations of en-echelon quartz vein generations at locality 7. The white square is 10x10cm. (top right) Sketch figure of veins at top left showing the observed veins and their relative age relationships as well as the orientation of fibrous quartz crystals within the veins shown as black lines. Blue is oldest, Orange is intermediate age, Green is youngest. The veins reflect an anti-clockwise rotation of top-to-SE with relative age.

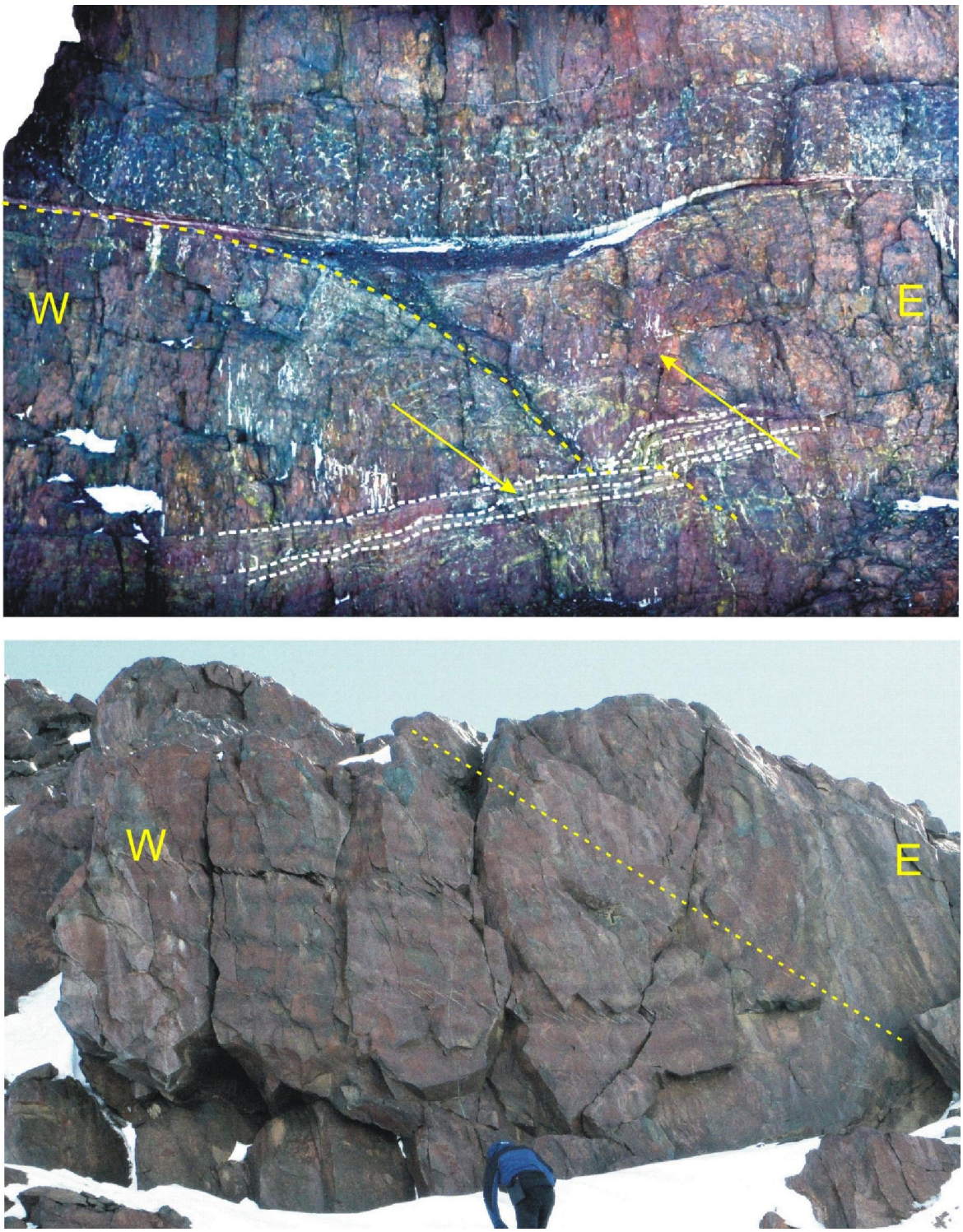

Figure 10. Photographs of structures recorded in the Straumsnutane area at locality 114 (Figure 4). (above) View northwards at the southern end of Snokallen showing a thrust fault with top to the west geometry. Note the sediment and pillow lava layers at the top of the sequence are unaffected by the faulting suggesting that the faulting was syn-depositional. This locality is similarly described and interpreted by Spaeth (1987). (below) Photograph viewed facing north of a synclinal fold defined by layered basaltic andesite at nunatak 1090 (Figure 4) with top to the west vergence. Note the inclined axial planar fabric preferentially developed in some layers. Dashed line is an inferred axial plane.

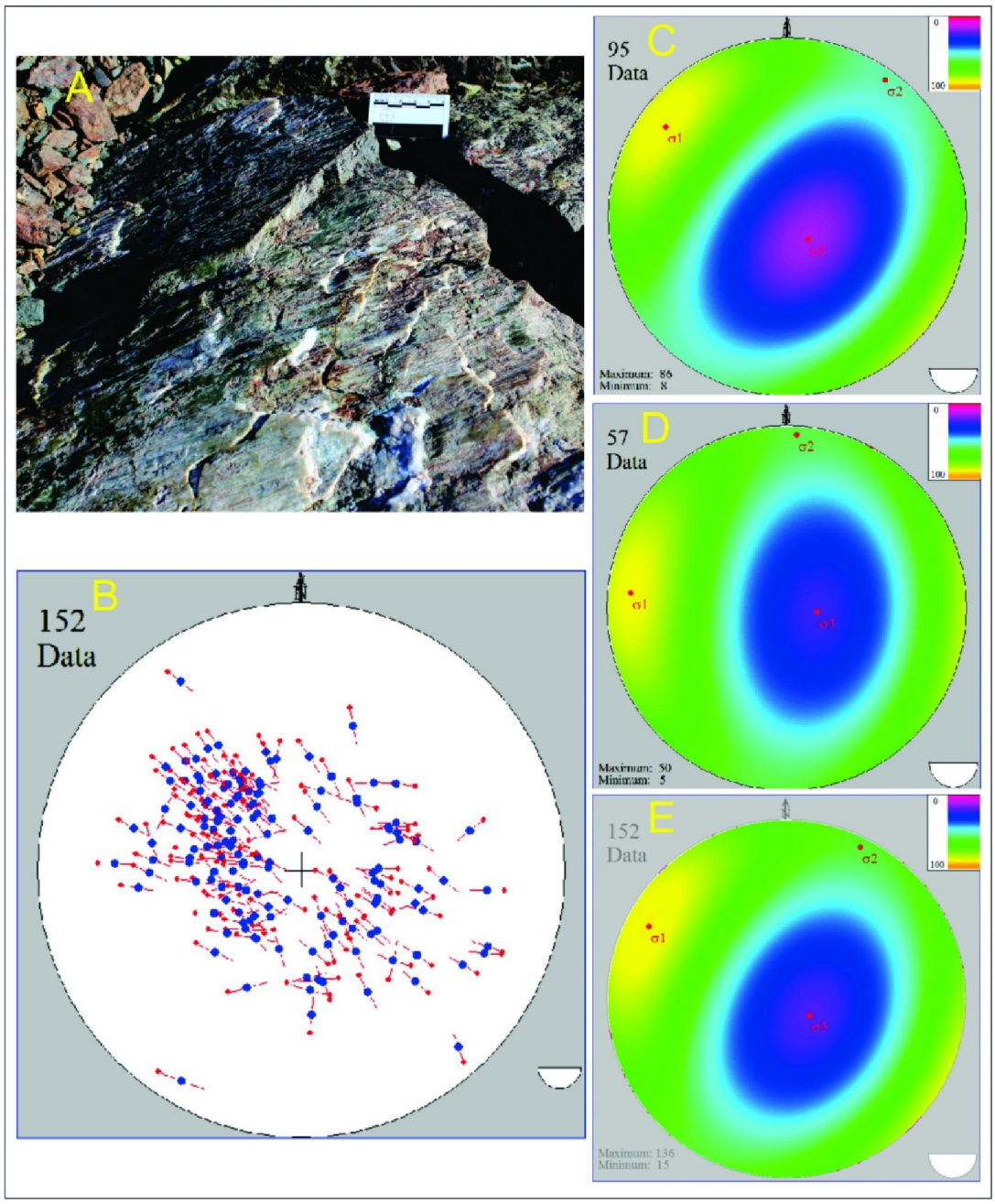

Figure 11.(a) Photograph of an epidote-coated slickensided fault surface with strong lineations typical of many of the planes seen in Straumsnutane. (b – e) Stereographic projections summarising the orientation of paleostress interpreted from slickensided fault plane data using Fabric 8 software. (b) Hoeppener diagram showing orientation data from the entire area. The diagram shows poles to slickensided fault planes (blue dots) and the direction of slip of the hanging wall (red arrows). (c-e) Paleostress reconstructions using right dihedral analysis. Cool (blue-purple) colours indicate low stress concentrations; warm (yellow) colours high stress concentrations: (c) Data from the eastern region of the study area (σ_1= 14°/327°; σ_2= 12°/004°; σ_3=72°/116°). (d) Data from the western region of the study area (σ_1= 17°/294°; σ_2= 12°/028°; σ_3=74°/140°). (e) Combined data from the entire Straumsnutane area (σ_1= 20°/303°; σ_2= 12°/038°; σ_3=72°/148°).

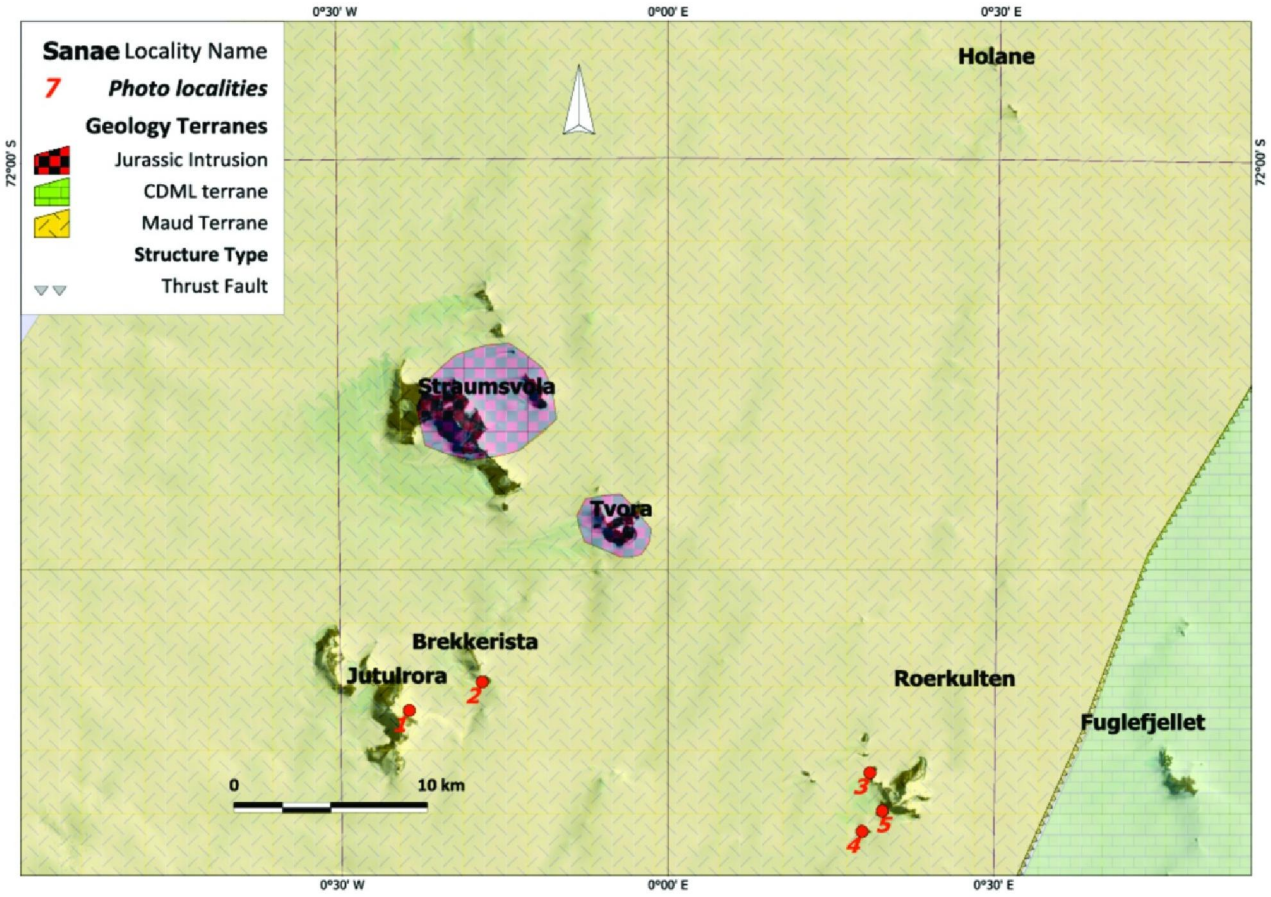

Figure 12. Map showing western Sverdrupfjella and the names of the various nunataks mentioned in the text and localities where field photos were recorded. The location of this map in Figure 3 shows its extent in western Sverdrupfjella.

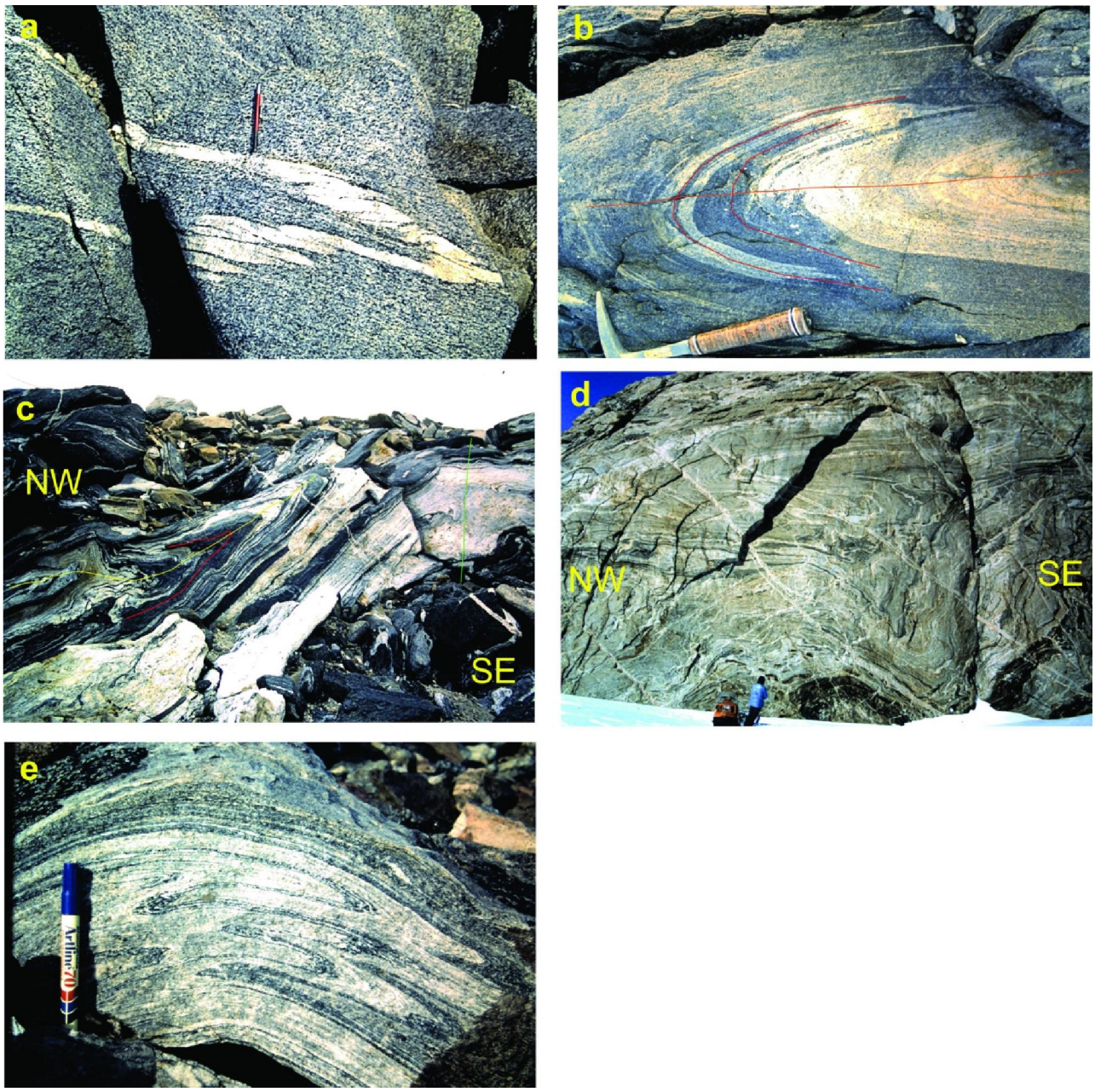

Figure 13.Field exposures of structures at various localities in western Sverdrupfjella. (a) Near recumbent tight F_1 fold defined by a migmatitic vein in hbl-bt-qtz-feldspar gneiss. Note the axial planar foliation. (b) Tight recumbent isoclinal F_2 fold, refolding an F_1 fold defining a Type 3 interference fold pattern after Ramsay (1967, p531.) Axial traces of the F_1 and F_2 folds are shown in red as well as the F_2 axial plane in yellow. (c) A tight isoclinal F_1 fold at centre left (axial plane in red) refolded by a similarly oriented F_2 fold (axial plane in yellow) in which the whole structural train is refolded around a F_3 fold with ca. vertical axial plane at right (green). The height of exposure is ca. 2m. (d) Partially exposed F_3 upright antiformal fold at bottom centre defined by a mafic vein at Roerkulten (locality 5 in Figure 12). Note the SE dipping granitic veins and the strong F_2 NW vergent folding above the mafic vein. Person for scale. (e) Tight recumbent isoclinal F_2 folds in finely banded gneiss refolded over a F_3 open fold.

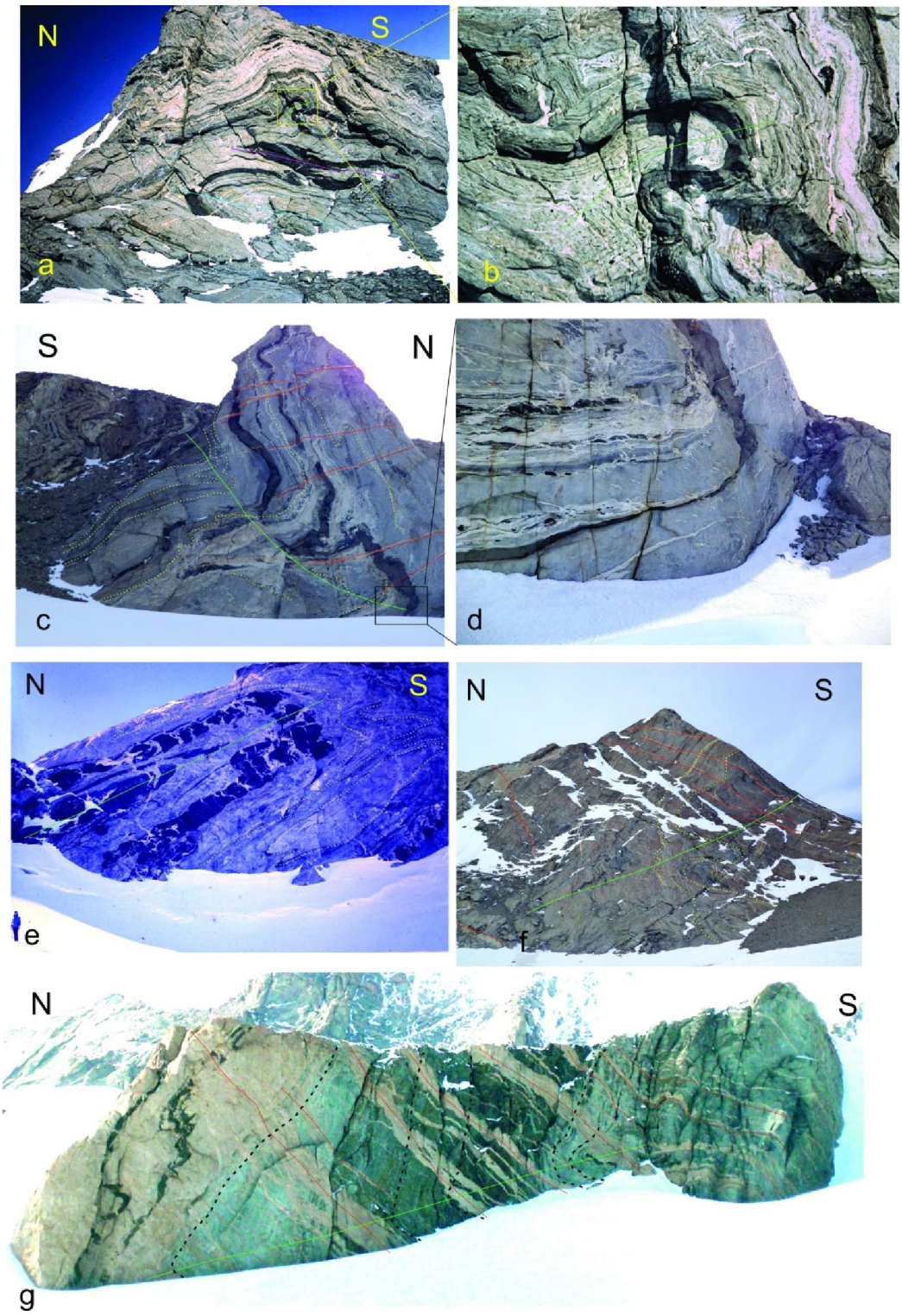

Figure 14. Field exposures of structures at various localities in western Sverdrupfjella. (a) Exposure at Jutulrora (Figure 12) showing the relative orientations of axial planes for F_1 (purple line), F_2 (blue line) and F_3 folds (green line). (b) an enlargement of the axial plane of the F_3 fold in (a). Height of exposure is ca. 200m. (c) Asymmetric synformal fold with south to southeast vergence at Jutulrora (photo locality 1 in Figure 12) Structural data from this locality are shown in Figure 15a. Note the N dipping axial plane and the south dipping Dalmatian Granite veins as red lines showing dilation ~perpendicular to the axial plane. (d) Enlarged insert of the fold hinge zone in the box area of Figure 14c. Note the axial planar lenticular leucosomes. (e) S vergent isoclinal inclined fold at Roerkulten (photo locality 4 in Figure 12). Note the dilation vein orientation of the inter-mafic boudins oriented perpendicular to the axial plane. Fold data from this locality are shown in Figure 15d. (f) Asymmetric synformal fold with southward vergence at Brekkerista (photo locality 2 in Figure 12) Axial planar trace is shown in green. South dipping granitic veins are shown in red. Fold data from this locality are shown in Figure 15b. (g) Asymmetric recumbent fold with south to southeast vergence at Roerkulten and shallow NW dipping axial plane. Cliff height is ca. 100m. Structural data from this locality are shown in Stereonet 15c and the locality is photo locality 2 in Figure 12. Note the SE dipping pegmatitic veins shown in red and the axial planar trace shown in green with the fold closure just above the snow line lower left.

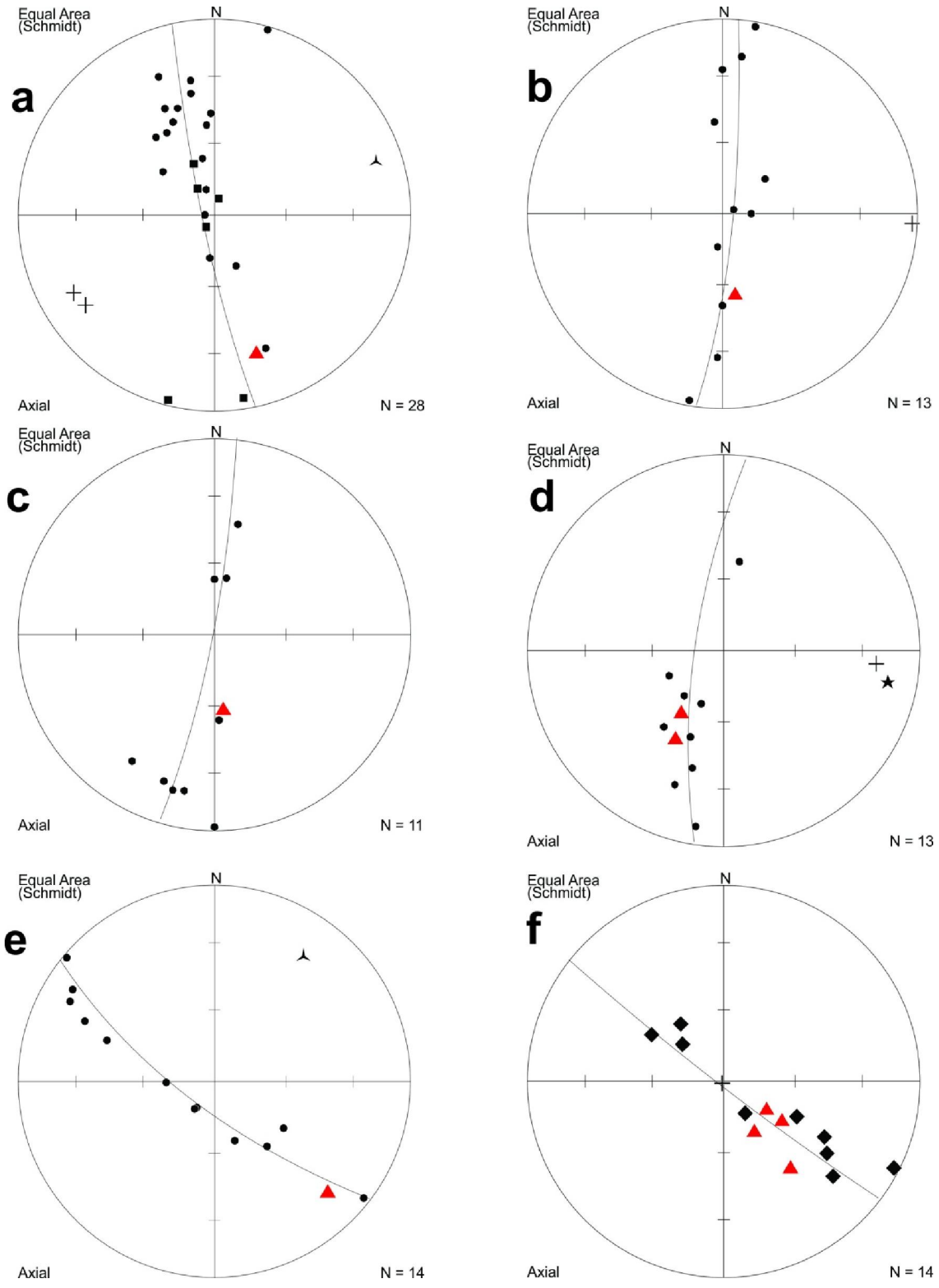

Figure 15. Stereographic projections summarising structural data from various localities. Abbreviations are $FAF_{2=}$ Fold axis F2, So+S1= primary and F1 planar fabrics, APF1 = axial plane F1 fold, APF2 = axial plane F2 fold L3= Lineation D3 (a) Structural data from Jutulrora (photo locality in Figure 13) and Figure 14c and d (b) structural data from Brekkerista (photo locality in Figure 12) and field photo Figure 14f.(c) Structural data from Roerkulten photo locality in Figure 12 and field photo Figure 14g. (d) Structural data from fold at Roerkulten photo locality 4 in Figure 12 and field photo Figure 14e. (e) Structural data from Roerkulten photo locality 5 in Figure 12. The data represent planar fabrics in gneiss with the red triangle a measured NW dipping axial plane. (g) Structural data from Roerkulten photo locality 5 in Figure 12. The black diamond data represent the contact of an intrusive amphibolite dyke, and the red triangles representing NW dipping measured axial planar foliations in the amphibolite.

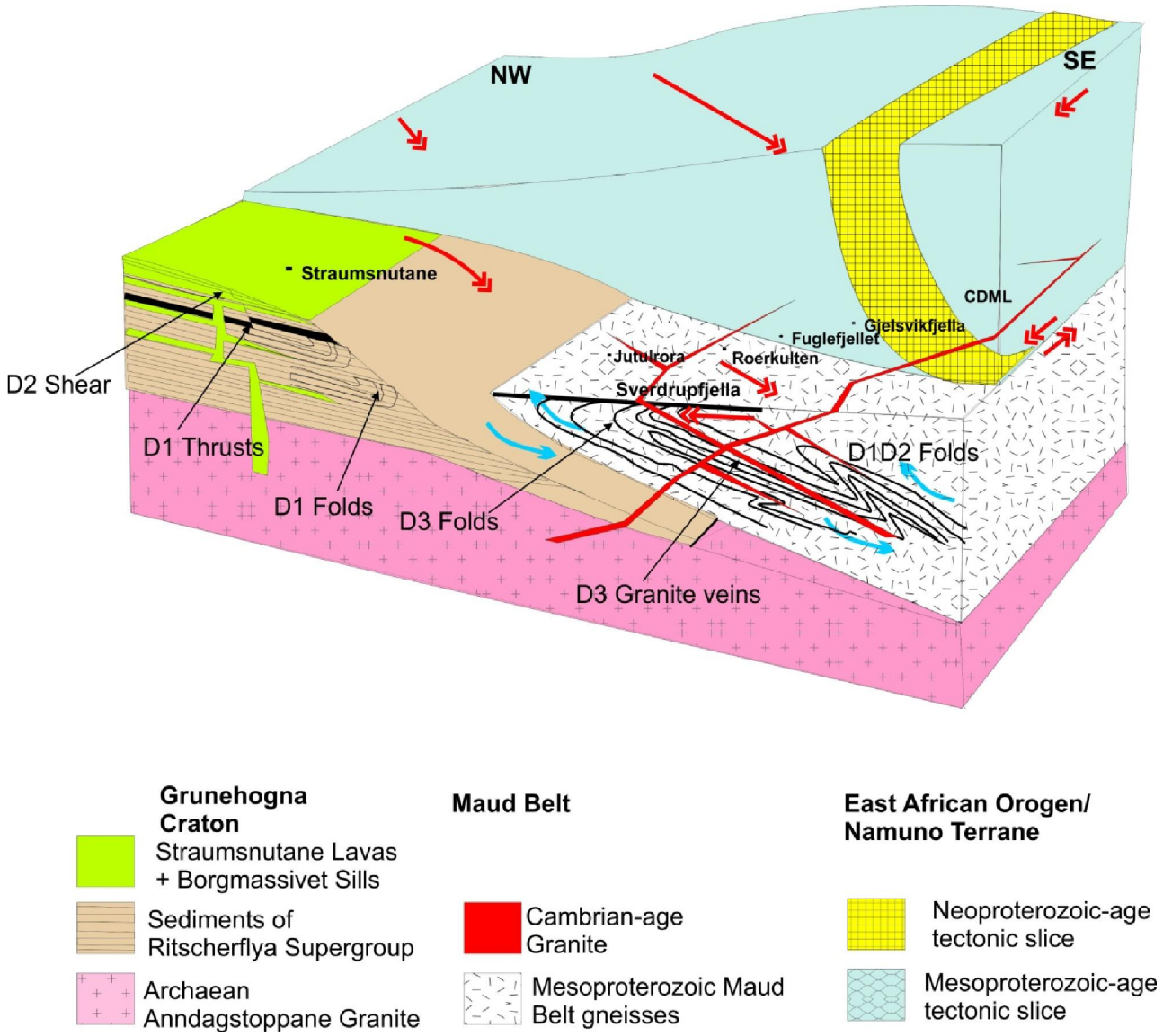

Figure 16. Tectonic schematic interpretation of the relationships between the Grunehogna Craton, the Maud Belt and the EAO Namuno-nappe structure. Single-headed blue arrows reflect senses of shear between different blocks related to D_1. Double-headed red arrows reflect inferred senses of shear between different blocks related to $D_{2/3}$. The types of structures observed with inferred deformational age are shown as well as relative schematic location in the section of geographic localities reported in the text.

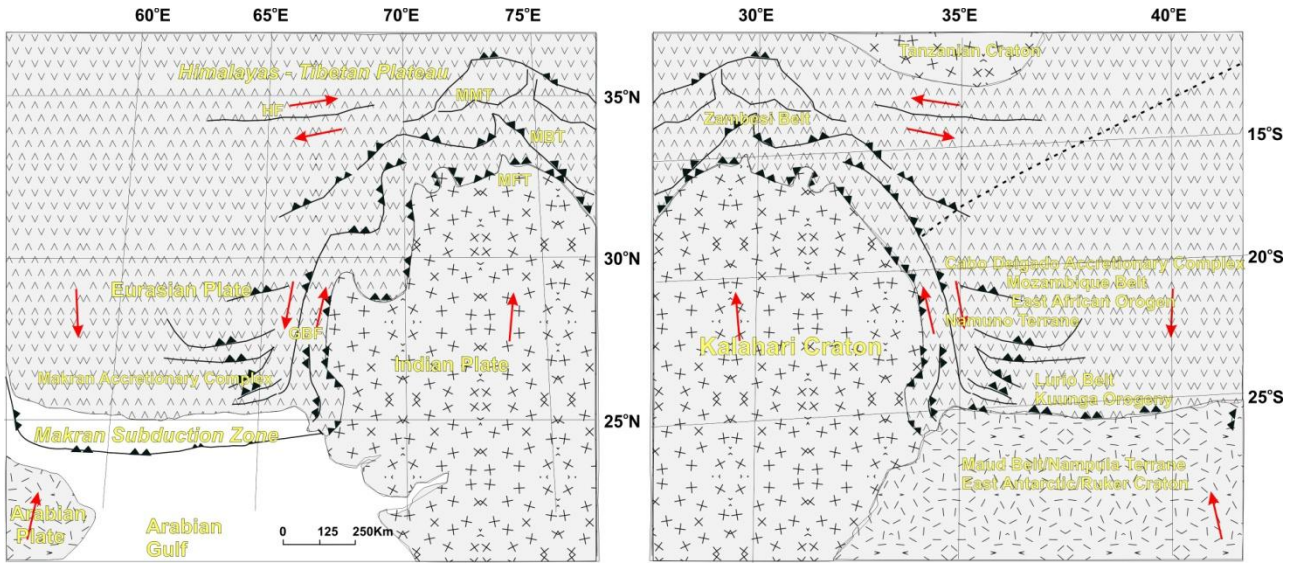

Figure 17. (a left) Figure showing plates and major structures associated with the collision between Eurasia in the north and India and Arabia in the south with the latter plates being subducted under Eurasia. Structure names and configuration are from Crupa et al., (2017). MBT=Main Boundary Thrust. HF=Heart Fault. MFT= Main Frontal Thrust. MMT=Main Mantle Thrust. GBF=Ghazban Fault. (b right) Modified mirror image of Figure 15a showing an inferred schematic similar configuration reflecting the Kuunga Orogeny collision between the Kalahari Craton (southern Gondwana) and the Tanzanian Craton (northern Gondwana) along the Damara-Zambesi-Lurio belts. The dashed line reflects the approximate current day position of the Lurio suture under the hanging wall block.